

## Surface effects on spinodal decomposition in binary mixtures and the interplay with wetting phenomena

Sanjay Puri\* and Kurt Binder

*Institut für Physik, Johannes Gutenberg-Universität Mainz, D-55099 Mainz, Germany*

(Received 16 November 1993)

The phase separation of binary mixtures in a semi-infinite geometry is investigated both by a phenomenological theory and by numerical calculations using a discrete equivalent of the descriptive equations. In the framework of “model B” (which describes solid binary mixtures), attention is paid to a proper treatment of the boundary conditions at the free surfaces. We confine ourselves to short-range surface forces and consider parameter values that correspond to both nonwet and wet surfaces in thermal equilibrium. During the initial stages of spinodal decomposition, after a quench from considering an initial condition that corresponds to a completely random concentration distribution, one finds a rather rapid growth of a thin surface enrichment layer of the component that is energetically preferred by the surface. This layer stabilizes a growing concentration wave in the direction normal to the surface, whose oscillations are damped to zero as one goes into the bulk. Studying concentration correlations in the direction parallel to the surface at a distance  $z$  from it, one can define a length scale  $l_{\parallel}(z, t)$  describing the coarsening of the growing domains. We find that  $l_{\parallel}(z, t) \approx A(z) + B(z)t^a$  for large  $t$ , with an amplitude  $B(z)$  that increases as  $z \rightarrow 0$  and an exponent  $a$  which is close to that for Lifshitz-Slyozov growth, viz.,  $a \approx \frac{1}{3}$ . This increase is due to an orientation of the growing elongated domains parallel to the surface near  $z = 0$ . There is surprisingly little influence of the wetting transition on these phenomena—even for a wet surface the growth of the wetting layer is only logarithmic in time for short-range surface forces, and hence does not significantly affect phenomena on the faster time scales of spinodal decomposition. Experimental findings on the interplay of spinodal decomposition and wetting are critically discussed.

PACS number(s): 68.45.Gd, 81.30.Mh, 64.75.+g

### I. INTRODUCTION AND OVERVIEW

In recent years there has been an enormous interest—both theoretical and experimental—in the equilibrium aspects of surface effects on phase transitions [1–14]: in a thin film geometry, surface effects may lead to a shift of the transition away from parameters where it occurs in the bulk (e.g., “capillary condensation” of fluids confined between plates [1–3]); in a semi-infinite geometry, surfaces may lead to a change of the critical behavior locally near the surface for second-order transitions [4,5], or to surface-induced ordering or disordering for first-order transitions [12,13] (e.g., “surface melting” [13,14]). These phenomena can also be interpreted as wetting phenomena [6–10], i.e., a phase transition of the surface (excess) free energy where an interface (between coexisting phases) unbinds from the surface.

Much less is known about the kinetics of such ordering phenomena under the influence of surfaces, and this is the problem addressed in this paper. Very recent experiments studying the kinetics of unmixing of thin films of small molecule fluid mixtures [15], polymer solutions [16], and polymer blends [17–20] have yielded a wealth of unexplained details with regard to the interplay of spi-

nodal decomposition [21–24] and wetting, and clearly a detailed theoretical analysis of such phenomena is very interesting. Since the pioneering work of Cahn and Hilliard [24] spinodal decomposition in the bulk has been studied extensively (see Refs. [21–23] for reviews) and also the growth kinetics of wetting layers has been considered occasionally [25–31]. However, the latter work almost always deals with systems having a nonconserved order parameter, and hence is inapplicable to binary mixtures where the order parameter (concentration difference between the average concentration and the critical concentration) is conserved. Recent studies considering surface effects on spinodal decomposition [32,33] have used an *ad hoc* boundary condition at the surface, which is clearly not at all suitable for a consistent incorporation of wetting phenomena. However, for studying surface effects on the dynamics of concentration fluctuations in mixtures a correct treatment of the boundary conditions at the surface is crucial.

The problem has recently been addressed [34–36] considering an Ising-lattice model of a binary mixture and deriving the dynamic boundary conditions at a hard wall from the master equation for a Kawasaki [37] direct exchange model in mean-field approximation. Gratifyingly, near the critical point of the mixture essentially equivalent result have been obtained thereafter [38] from a much more general approach using symmetry considerations only. These dynamic boundary conditions (in the form of Ref. [36]) are used in the present work and this should allow, in our opinion, a reliable study of the

\*Permanent address: School of Physical Sciences, Jawaharlal Nehru University, New Delhi 110067, India.

interplay between spinodal decomposition and wetting.

Nevertheless we add a caveat with respect to the applicability of our results to recent experiments [15–20]. Our model is qualitatively correct for solid mixtures, see Sec. II (“model *B*” in the Hohenberg-Halperin [39] classification), while fluid mixtures require the inclusion of hydrodynamic interactions (“model *H*” [39]) which have a pronounced effect on the dynamics of spinodal decomposition, both at intermediate [40] and late [41–44] stages of the growth. Secondly, the present paper considers semi-infinite systems only rather than systems confined between two walls, whose distance is comparable to the characteristic domain size at late stages. This situation (occurring often in experiments [15–20]) will be considered in a separate publication [45]. While there is ample experimental evidence that hydrodynamic mechanisms control bulk phase separation kinetics of near-critical mixtures of both small molecules [21–23,46] and polymers [22,47,48], it also appears that they are quite relevant in the thin film geometry [15–20].

This paper is organized as follows. In Sec. II we define our model and introduce the notation. Section III recalls the basic equilibrium properties of semi-infinite mixtures, including the wetting phase diagram of our model and the dynamics of surface enrichment and initial stages of spinodal decomposition in the linearized approximation. Section IV presents numerical results for the intermediate and late stages of spinodal decomposition near a surface. Section V summarizes our conclusions.

## II. DISCUSSION OF THE BASIC MODEL

Let us restrict attention for the moment to a model of a binary (*AB*) mixture in contact with a surface and with pairwise interactions  $\varphi_{AA}, \varphi_{AB}, \varphi_{BB}$  between atoms at sites  $\mathbf{r}_i, \mathbf{r}_j$ . In terms of local concentration variables  $c_i = 1$  if site  $i$  is occupied by an *A* atom and  $c_i = 0$  if it is occupied by a *B* atom. The Hamiltonian is (cf. Fig. 1; sums over pairs run over all pairs once, and lattice sites exist in the positive half space  $z > 0$  only)

$$\begin{aligned} \mathcal{H} = & \sum_{i \neq j} [c_i c_j \varphi_{AA}(\mathbf{r}_i, \mathbf{r}_j) + c_i (1 - c_j) \varphi_{AB}(\mathbf{r}_i, \mathbf{r}_j) \\ & + (1 - c_i) c_j \varphi_{AB}(\mathbf{r}_i, \mathbf{r}_j) \\ & + (1 - c_i)(1 - c_j) \varphi_{BB}(\mathbf{r}_i, \mathbf{r}_j)] \\ & + \sum_i [v_A(\mathbf{r}_i) c_i + v_B(\mathbf{r}_i)(1 - c_i)]. \end{aligned} \quad (1)$$

Here  $v_A(\mathbf{r}_i)$  [ $v_B(\mathbf{r}_i)$ ] are forces exerted on *A* (*B*) atoms at site  $\mathbf{r}_i$  due to the hard wall at  $z=0$ . In the case of a free surface (against vacuum or air) at  $z=0$  it would seem natural to set  $v_A(\mathbf{r}_i) = v_B(\mathbf{r}_i) = 0$ , of course: but in this case any intrinsic roughness of the interface between the mixture and the “vapor phase” at  $z < 0$  is disregarded, and the following treatment would hold for solids above their roughening transition temperature  $T_R$  [49,50] (and for fluid mixtures where the fluid-gas interface always is rough, of course) only on length scales distinctly larger than the scale of this atomic roughness. A second effect due to the breaking of the translational symmetry of the

surface is that, in general, one must expect that the pairwise interactions  $\varphi_{AA}, \varphi_{AB}, \varphi_{BB}$  not only depend on the relative distance  $\mathbf{r}_i - \mathbf{r}_j$ , but also on  $\mathbf{r}_i, \mathbf{r}_j$  separately (e.g., different interactions  $\varphi_{AA}^S, \varphi_{AB}^S, \varphi_{BB}^S$  occur if both sites  $i, j$  are in the layer right adjacent to the surface [4,51]).

Of course, we are not interested here in the “correct” description of atomistic detail, but rather Eq. (1) (and Fig. 1) only serve as a generic model to derive a reasonable continuum description which holds for a much larger class of systems [4–6,34]. Thus we simplify the problem by restricting the range of all interactions to nearest neighbors, and take all interactions  $\varphi_{AA}, \varphi_{AB}, \varphi_{BB}$  to be independent of their sites  $i, j$  except if both sites are in the surface layer  $n=1$ . Finally, we also assume  $v_A(\mathbf{r}_i), v_B(\mathbf{r}_i)$  to be nonzero only if  $i$  is in the layer  $n=1$ . This latter assumption, however, means that we restrict attention to wetting with short-range forces, and it is well known that this situation differs in important qualitative respects from wetting with long-range forces [6], e.g., van der Waals forces which decay proportional to  $z^{-3}$  with the distance  $z$  from the surface. This restriction of our model is one more reason why one should not make too hasty conclusions about experimental implications of our results, but we feel that one must understand the simpler short-range case first before one can discuss the case of long-range surface forces.

It is convenient to translate the model into the Ising spin representation [4] via the transformation

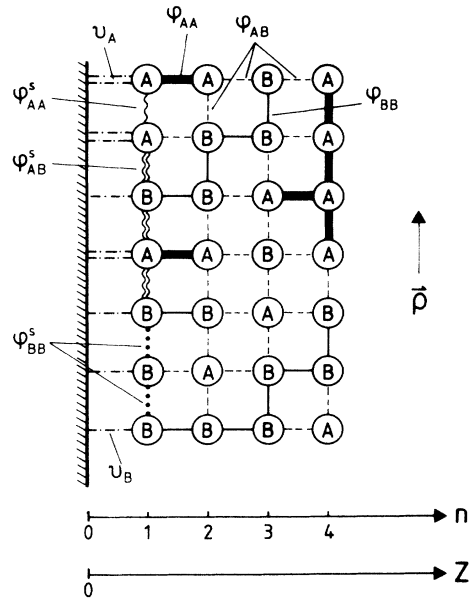


FIG. 1. Schematic picture of the surface of a binary (*AB*) alloy at  $z=0$  (the shading indicates that this may represent an inert hard wall). Different atoms (circles) and nearest-neighbor interactions between them (and the wall) are indicated by different types of lines. For a discrete description, lattice planes parallel to the surface are labeled by a positive integer  $n$ , while in the continuum description coordinates parallel ( $\rho$ ) and perpendicular ( $z$ ) to the surface are used as indicated.

$c_i = (1 - S_i)/2$  ( $S_i = \pm 1$ ) which yields

$$\mathcal{H} - \sum_i c_i \mu_A - \sum_i (1 - c_i) \mu_B = - \sum_{\langle i,j \rangle} J_{ij} S_i S_j - H \sum_i S_i - H_1 \sum_{i \in \text{1st layer}} S_i + \mathcal{H}_0, \quad (2)$$

where  $\mu_A, \mu_B$  are the chemical potentials of both species, and  $\mathcal{H}_0$  is a constant which only affects the energy scale. The pairwise “exchange” interaction  $J_{ij}$  is

$$J_{ij} = J = \frac{1}{2} \varphi_{AB} - \frac{1}{4} (\varphi_{AA} + \varphi_{BB}), \quad (3)$$

when at least one of the sites  $i, j$  is not in the surface layer  $n = 1$ . If both sites are in the layer  $n = 1$ , we have

$$J_{ij} = J_S = \frac{1}{2} \varphi_{AB}^S - \frac{1}{4} (\varphi_{AA}^S + \varphi_{BB}^S). \quad (4)$$

The bulk “magnetic field”  $H$  is (for sites  $i$  not in the  $n = 1$  layer)

$$H = \frac{1}{2} (\mu_B - \mu_A) + \frac{1}{2} \sum_{j(\neq i)} (\varphi_{AA} - \varphi_{BB}), \quad (5)$$

while for sites  $i$  from the first layer we have an additional “surface field”  $H_1$ ,

$$H + H_1 = \frac{1}{2} (\mu_B - \mu_A + v_B - v_A) + \frac{1}{2} \left[ \sum_{\substack{j(\neq i) \\ j \in \text{1st layer}}} (\varphi_{AA}^S - \varphi_{BB}^S) + \sum_{j \in \text{2nd layer}} (\varphi_{AA} - \varphi_{BB}) \right]. \quad (6)$$

At this point we emphasize that a nonzero surface field  $H_1$  arises even for the case where  $v_B = v_A = 0$  and interactions are unchanged near the surface, i.e.,  $\varphi_{AA}^S = \varphi_{AA}$  and  $\varphi_{BB}^S = \varphi_{BB}$ , as long as  $\varphi_{AA} - \varphi_{BB} \neq 0$ . This is a result of the “missing neighbors” of sites in the first layer. Considering the most symmetric case where also  $\varphi_{AA} = \varphi_{BB}$  clearly has little physical relevance for actual mixtures. While the “bulk field” in Eq. (2) is easily eliminated from the problem by fixing the average concentration

$$\bar{c} = \frac{1}{N} \sum_i \langle c_i \rangle, \quad (7)$$

which is also the concentration  $c_b$  in the bulk of our semifinite system, the additional surface field  $H_1$  must remain as a parameter in the problem. As is well known [4–11], this term is responsible for both surface enrichment and wetting phenomena in mixtures.

The simplest way of introducing dynamics into the model of Eq. (1) that respects the facts that (a) the concentration in the mixture is conserved and (b) the atomic mobility is due to local hopping events, is achieved by the Kawasaki [37] spin-exchange model. Again we emphasize that the aim is not an atomistically realistic description of solid alloys (which would require us to con-

sider the vacancy mechanism for the interdiffusion of the atomistic species [52–55] rather than a direct exchange mechanism), but the motivation of a reasonable coarse-grained continuum model. At this point, the treatment gets restricted to solids due to the complete neglect of transport via flow. Of course, even for very viscous systems such as polymer mixtures, it is now well established that hydrodynamic mechanisms control interdiffusion [56,57], and thus we do not claim that our treatment applies to such systems.

Treating the master equation for the Kawasaki model in a layerwise mean-field approximation [34–36] and transforming the resulting set of difference equations into a continuum description by expanding differences in the lattice coordinates in terms of differentials, one drives a partial differential equation for the bulk supplemented with two boundary conditions at the surface. The partial differential equation in the bulk is just the standard Cahn-Hilliard [24] equation

$$2\tau_s \frac{\partial \psi(\rho, z, t)}{\partial t} = -\nabla^2 \left[ \left( \frac{T_c}{T} - 1 \right) \psi(\rho, z, t) - \frac{1}{3} [\psi(\rho, z, t)]^3 + \frac{J}{T} \nabla^2 \psi(\rho, z, t) \right], \quad z > 0, \quad (8)$$

where  $\psi(\rho, z, t)$  is the continuum analog of the average of the spin  $\langle S_i(t) \rangle$  a time and  $\tau_s$  is the underlying time scale parameter of the spin-exchange model. In Eq. (8), the lattice spacing of Fig. 1 has been taken as unity, and we have kept only the terms of leading order near the critical point [concentration in the bulk  $c_B$  must be near  $c_B^{\text{crit}} = \frac{1}{2}$ , and the temperature  $T$  near the critical temperature  $T_c$ , which would be  $T_c = qJ/k_B$  in the mean-field theory for a (hyper) cubic lattice with coordination number  $q$ ]. Of course, the reason for considering the critical region is that the characteristic lengths of the problem (such as correlation lengths that appear in the concentration profile describing a surface enrichment layer or a wetting layer, or the critical wavelength that characterizes the linearized theory of spinodal decomposition [21–24]) are much larger than the lattice spacing. However, it is believed (as is usual in the critical phenomena [4–6,21,39]) that Eq. (8) is of much wider validity than its derivation suggests—especially if one treats the coefficients of the terms  $\psi$ ,  $\psi^3$ , and  $\nabla^2 \psi$  in the large square brackets of Eq. (8) as adjustable phenomenological parameters, and adds a random force term on the right-hand side to account for statistical fluctuations beyond the mean-field approximation [39].

Equation (8) is a differential equation of fourth order in  $\psi(\rho, z, t)$  and hence needs to be complemented with two boundary conditions at the surface  $z = 0$  (two other boundary conditions occur for  $z \rightarrow \infty$  which are not of much interest here). These boundary conditions are [34–36]

$$2\tau_s \frac{\partial \psi(\rho, z=0, t)}{\partial t} = \frac{H_1}{T} + \frac{J}{T} \left[ (q-2) \frac{J_s}{J} - (q-1) \right] \psi(\rho, z=0, t) - \left[ \frac{T_c}{T} - 1 - \frac{J}{T} \right] \frac{\partial \psi(\rho, z, t)}{\partial z} \Big|_{z=0} - \frac{1}{2} \left[ \frac{T_c}{T} - 1 + \frac{J}{T} \right] \frac{\partial^2 \psi(z, t)}{\partial z^2} \Big|_{z=0} - \frac{1}{6} \left[ \frac{T_c}{T} - 1 + \frac{5J}{T} \right] \frac{\partial^3 \psi(z, t)}{\partial z^3} \Big|_{z=0}, \tag{9}$$

and

$$\frac{\partial}{\partial z} \left[ \left[ \frac{T_c}{T} - 1 \right] \psi(\rho, z, t) - \frac{1}{3} [\psi(\rho, z, t)]^3 + \frac{J}{T} \frac{\partial^2}{\partial z^2} [\psi(\rho, z, t)] \right] \Big|_{z=0} = 0. \tag{10}$$

Equation (10) simply describes the fact that the concentration current in the direction normal to the surface must vanish for  $z=0$ , which acts as an impenetrable wall. While this equation can be trivially postulated, the first equation [Eq. (9)] is of greater interest since it characterizes the effects of the surface as a result of (a) the change of interactions near the surface ( $J_s \neq J$ ); (b) the “surface field”  $H_1$ ; and (c) the one-sided gradients due to the absence of material in the  $-z$  direction. Since these terms are not diffusive but of a simple relaxational type, it is clear that this boundary condition has the effect of rapidly driving the local order parameter at the surface to a value dictated by the static equilibrium at the surface.

We now restrict attention to  $T < T_c$  where the homogeneous mixture is thermodynamically unstable) and introduce a rescaling of parameters in terms of the bulk correlation length  $\xi_b$ , which is

$$\xi_b = [2q(1 - T/T_c)]^{-1/2}. \tag{11}$$

Our rescaling takes the form

$$Z = z/(2\xi_b), \quad \mathbf{R} = \rho/(2\xi_b), \tag{12a}$$

$$\tau = \frac{(T_c/T - 1)}{8\tau_s \xi_b^2} t \xrightarrow{T \rightarrow T_c} (16q\tau_s \xi_b^4)^{-1} t, \tag{12b}$$

$$h_1 = \frac{4H_1}{\sqrt{3}T} (T/T_c)^{3/2} (2q)^{3/2} \xi_b^5, \tag{12c}$$

$$g = 8 \left[ (q-2) \frac{J_s}{J} - (q-1) \right] \xi_b^4, \tag{12d}$$

$$\phi(\mathbf{R}, Z, \tau) = \frac{\psi(\mathbf{R}, Z, \tau)}{\psi_0}, \quad \text{where } \psi_0 = \sqrt{3(T_c/T - 1)}. \tag{12e}$$

As an abbreviation we also use  $\gamma = 4\xi_b^3$  and then the rescaled partial differential equation reads ( $\nabla$  is now a gradient operator referring to derivatives with respect to  $Z$  and  $\mathbf{R}$ ), for  $Z > 0$ ,

$$\frac{\partial \phi(\mathbf{R}, Z, \tau)}{\partial \tau} = -\nabla^2 \left\{ \phi(\mathbf{R}, Z, \tau) - [\phi(\mathbf{R}, Z, \tau)]^3 + \frac{1}{2} \nabla^2 \phi(\mathbf{R}, Z, \tau) \right\}, \tag{13}$$

with the rescaled boundary conditions

$$\frac{\partial \phi(\mathbf{R}, Z=0, \tau)}{\partial \tau} = h_1 + g\phi(\mathbf{R}, Z=0, \tau) + \gamma \frac{\partial \phi(\mathbf{R}, Z, \tau)}{\partial Z} \Big|_{Z=0} - \left[ \frac{\gamma}{4} \right]^{2/3} \frac{\partial^2 \phi(\mathbf{R}, Z, \tau)}{\partial Z^2} \Big|_{Z=0} - \frac{5}{6} \left[ \frac{\gamma}{4} \right]^{1/3} \frac{\partial^3 \phi(\mathbf{R}, Z, \tau)}{\partial Z^3} \Big|_{Z=0} \tag{14}$$

and

$$\frac{\partial}{\partial Z} \left\{ \phi(\mathbf{R}, Z, \tau) - [\phi(\mathbf{R}, Z, \tau)]^3 + \frac{1}{2} \nabla^2 [\phi(\mathbf{R}, Z, \tau)] \right\} \Big|_{Z=0} = 0. \tag{15}$$

The rescaling of time in Eq. (12b) simply expresses the “critical slowing down” of “model B” (with a dynamic critical exponent equal to 4 in mean-field theory [39]). It is seen that the rescaling has the effect that the bulk equation is not only formulated entirely in terms of dimensionless quantities but also is free of any system-dependent parameters, while such parameters ( $h_1, g, \gamma$ ) still appear in the first boundary condition, Eq. (14). This reflects the fact that even in the region near bulk criticality where the behavior after rescaling reflects the universal bulk behavior of “model B” [39] we have the possibility of nontrivial surface phase behavior (such as wetting transitions). This will be briefly summarized in the next section.

In principle, Eq. (13) should be supplemented by a random noise term expressing the statistical fluctuations: At any nonzero temperature, these fluctuations will have some effect on spinodal decomposition, particularly during the early and intermediate stages of the growth. In fact, these fluctuations are very important if we consider rescaled times of order unity, but are rather unimportant for the scaling behavior in the late stages of growth [22,23,42–44,60–62]. Such fluctuations would be included if one performs Monte Carlo simulations directly on

the Kawasaki spin-exchange model corresponding to Fig. 1 [63]. However, the advantage of the cell-dynamics approach clearly is that effectively much larger length scale of the discretization of Eq. (13) is of the same order as the correlation length, and hence much larger than the lattice spacing. In turn, the advantage of the Monte Carlo methods [21,22,54,55,62,63] would be that temperatures also below the roughening transition temperature [49,50] would be accessible—where wetting (Fig. 2) is replaced by a sequence of layering transitions [4,6,64]—while Eq. (13) cannot describe layering.

### III. THEORETICAL BACKGROUND

#### A. Static surface properties of semi-infinite mixtures and the wetting phase diagram

As discussed in [4–10], the static properties of the model described by Eqs. (1)–(6) in the continuum approximation can be described in terms of a free energy functional

$$\frac{\Delta\mathcal{F}}{k_B T_c} = \int d\mathbf{R} \left[ \int_0^\infty dZ \frac{1}{2} \left( \frac{1}{2} (\nabla\phi)^2 - \phi^2 + \frac{1}{2} \phi^4 \right) - \frac{h_1}{\gamma} \phi_1 - \frac{1}{2} \frac{g}{\gamma} \phi_1^2 \right], \quad (16)$$

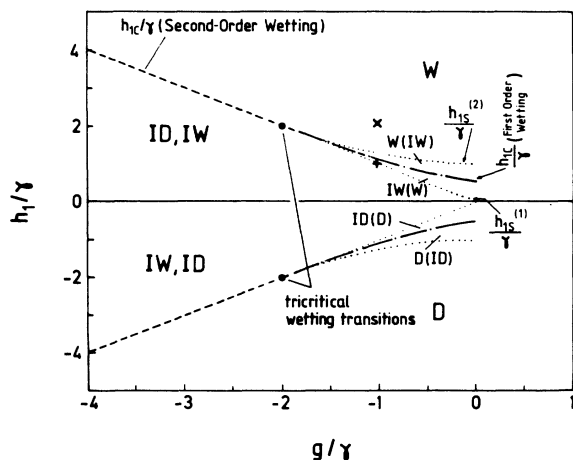


FIG. 2. Phase diagram for the phenomenological model of Eq. (16) for wetting and drying. The states are labeled as wet (W), incompletely wet (IW), dry (D), and incompletely dry (ID). Note that the phase diagram is symmetric around the abscissa  $h_1/\gamma = 0$  if one interchanges the role of wet and dry states, respectively. For  $g/\gamma < -2$  the transition is a second-order wetting transition (broken straight lines) at  $h_{1c}/\gamma$  which ends at the wetting tricritical point ( $g_i/\gamma = -2$ ,  $h_{1i}/\gamma = \pm 2$ ). Dash-dotted curves denote first-order wetting transitions, dotted curves denote “surface spinodals” [stability limits of metastable wet (dry) or incompletely wet (dry) phases, respectively]. These stability limits are given by the equations  $h_{1s}^{(1)}/\gamma = -g/\gamma$  (for  $g/\gamma > -2$ , lower spinodal) and  $h_{1s}^{(2)}/\gamma = 1 + (g/2\gamma)^2$  (for  $g/\gamma > -2$ , upper spinodal), in the upper half plane. The two crosses (+, x) denote the equilibrium states of the surface reached in our simulations of quenching experiments for times  $\tau \rightarrow \infty$ . (From Ref. [31].)

where  $\phi_1(\mathbf{R}) \equiv \phi(\mathbf{R}, Z=0)$  is the local order parameter at the surface, and we have invoked the same rescaling of parameters as in the preceding section, and consider the critical region where  $T \approx T_c$ .

The surface phase diagram that results from Eq. (16) has been discussed in previous work [27,31]. Figure 2 shows the phase boundaries in the plane of the variables  $h_1/\gamma$  and  $g/\gamma$ . These phase boundaries result from minimizing the free energy functional Eq. (16), which yields an Euler-Lagrange equation [ $\phi(\mathbf{R}, Z)$  can be taken as being independent of  $\mathbf{R}$ ]

$$\phi(Z) - \phi^3(Z) + \frac{1}{2} \frac{\partial^2}{\partial Z^2} \phi(Z) = 0, \quad (17)$$

with the boundary condition

$$\frac{h_1}{\gamma} + \frac{g}{\gamma} \phi(Z=0) + \frac{\partial\phi(Z)}{\partial Z} \Big|_{Z=0} = 0. \quad (18)$$

Equations (17) and (18) are compatible with the static limit of Eqs. (14) and (15), of course [note that  $\gamma \rightarrow \infty$  near  $T_c$  and thus the higher-order gradient terms in Eq. (15) can safely be neglected in the static limit]. Note that for unchanged interactions at the surface ( $J_s = J$ ), near criticality ( $\xi_b \rightarrow \infty$ ) one has  $g/\gamma = -2\xi_b \rightarrow -\infty$ ,  $h_1/\gamma \propto H_1 \xi_b^2 \rightarrow \infty$ , i.e., typically one is in the region where the surface is wet far above the second-order wetting transition on the left-hand side of the phase diagram (for  $H_1 > 0$ ). However, since in a typical experimental situation one is interested in spinodal decomposition and wetting far from the bulk critical point, we shall use the present model for parameter choices of  $g$ ,  $h_1$ ,  $\gamma$  of order unity as well.

#### B. General formalism

Both surface critical phenomena [4–6] and wetting [6–10] can be discussed in terms of the singular behavior of the surface excess free energy density  $f_s(T, H, H_1)$ , which is conveniently defined from the free energy density  $f(T, H, H_1)$  of a thin film of thickness  $D$  with two equivalent surfaces

$$f(T, H, H_1) = f_b(T, H) + \frac{2}{D} f_s(T, H, H_1), \quad D \rightarrow \infty \quad (19)$$

$f_b(T, H)$  being the bulk free energy density of the considered system. Particularly interesting quantities are the response functions, e.g., the surface susceptibility  $\chi_s$  defined as

$$\begin{aligned} \chi_s &= - \frac{\partial^2 f_s(T, H, H_1)}{\partial H^2} \Big|_{T, H_1} \\ &= \sum_n (\chi_n - \chi_b) = \int_0^\infty dz [\chi(z) - \chi_b], \end{aligned} \quad (20)$$

where the bulk susceptibility is  $\chi_b = -[\partial^2 f_b(T, H)/\partial H^2]_T$ ; and the surface layer susceptibilities ( $m_n = \langle S_i \rangle_T$  with  $i$  being chosen from the  $n$ th layer)

$$\begin{aligned}\chi_1 &= - \left[ \frac{\partial^2 f_s(t, H, H_1)}{\partial H \partial H_1} \right]_T \\ &= \left[ \frac{\partial m_1}{\partial H} \right]_{T, H_1} = \sum_j (\langle S_i S_j \rangle_T - \langle S_i \rangle_T \langle S_j \rangle_T) / k_B T\end{aligned}\quad (21)$$

and

$$\begin{aligned}\chi_{11} &= - \left[ \frac{\partial^2 f_s(T, H, H_1)}{\partial H_1^2} \right]_{T, H} \\ &= \left[ \frac{\partial m_1}{\partial H_1} \right]_{T, H} \\ &= \sum_{j \in \text{1st layer}} (\langle S_i S_j \rangle_T - \langle S_i \rangle_T \langle S_j \rangle_T) / k_B T,\end{aligned}\quad (22)$$

where in Eqs. (21) and (22) the site  $i$  is chosen in the first layer. The layer magnetization  $m_n$  and the layer susceptibility  $\chi_n, \chi_{nn}$  are obvious generalizations to the case when a field  $H_n$  acts on spins in the  $n$ th layer only,

$$\chi_n = \left[ \frac{\partial m_n}{\partial H} \right]_{T, H_n} = \sum_j (\langle S_i S_j \rangle_T - \langle S_i \rangle_T \langle S_j \rangle_T) / k_B T, \quad i \in n \quad (23)$$

$$\chi_{nn} = \left[ \frac{\partial m_n}{\partial H_n} \right]_{T, H} = \sum_{j \in n} (\langle S_i S_j \rangle_T - \langle S_i \rangle_T \langle S_j \rangle_T) / k_B T, \quad i \in n. \quad (24)$$

Of course, Eqs. (23) and (24) are related to the long wavelength limits of the corresponding structure factors ( $\mathbf{k}_\parallel$  is a wave vector lying in a plane parallel to the surface)

$$S_n(\mathbf{k}) = \sum_j \exp[i\mathbf{k} \cdot (\mathbf{r}_j - \mathbf{r}_i)] (\langle S_i S_j \rangle_T - \langle S_i \rangle_T \langle S_j \rangle_T), \quad i \in n \quad (25)$$

$$\begin{aligned}S_{nn}(\mathbf{k}_\parallel) &= \sum_{j \in n} \exp[i\mathbf{k}_\parallel \cdot (\mathbf{r}_j - \mathbf{r}_i)] \\ &\times (\langle S_i S_j \rangle_T - \langle S_i \rangle_T \langle S_j \rangle_T), \quad i \in n.\end{aligned}\quad (26)$$

In analogy to Eq. (19) it makes sense to consider the surface excess  $S_s(\mathbf{k})$  of the total scattering intensity of a film,

$$S(\mathbf{k}) = S_b(\mathbf{k}) + \frac{2}{D} S_s(\mathbf{k}), \quad D \rightarrow \infty \quad (27)$$

where

$$S_s(\mathbf{k}) = \sum_n [S_n(\mathbf{k}) - S_b(\mathbf{k})] = \int_0^\infty dz [S(\mathbf{k}, z) - S_b(\mathbf{k})]. \quad (28)$$

In static equilibrium, the small  $k$  behavior of the structure factors defined via Eqs. (25)–(28) characterizes the typical length scales of the problem: for surface critical phenomena, it is simply the correlation length  $\xi_b$  which

controls these length scales for both the ordinary and special surface transition [4,5]. However, for critical wetting, correlation lengths  $\xi_\parallel, \xi_\perp$  in directions parallel and perpendicular to the surface need to be distinguished [6].

This phenomenology in equilibrium readily provides the appropriate theoretical framework to define the quantities which are needed to characterize surface effects on spinodal decomposition. In the nonequilibrium case, one again considers equal-time structure factors of the type defined in Eqs. (25)–(28), which now are time dependent since one considers quenching experiments far from thermal equilibrium. Thus the quantities that we wish to consider are [in a continuum description with  $\psi(\rho, z, t)$  as the time-dependent order parameter]

$$\begin{aligned}G_\parallel(\rho_1 - \rho_2, z, t) &= \langle \psi(\rho_1, z, t) \psi(\rho_2, z, t) \rangle \\ &\quad - \langle \psi(\rho_1, z, t) \rangle \langle \psi(\rho_2, z, t) \rangle\end{aligned}\quad (29a)$$

or its Fourier transform

$$S_\parallel(\mathbf{k}_\parallel, z, t) = \int d\rho \exp(i\mathbf{k}_\parallel \cdot \rho) G_\parallel(\rho, z, t). \quad (29b)$$

In Eqs. (29a) and (29b) the angular brackets denote averages over both initial conditions and thermal noise. We can also consider the more general correlation function

$$\begin{aligned}G(\rho_1 - \rho_2, z_1, z_2, t) &= \langle \psi(\rho_1, z_1, t) \psi(\rho_2, z_2, t) \rangle \\ &\quad - \langle \psi(\rho_1, z_1, t) \rangle \langle \psi(\rho_2, z_2, t) \rangle\end{aligned}\quad (30a)$$

and its counterpart in Fourier space (accounting for the breaking of translational symmetry by the wall)

$$\begin{aligned}S(\mathbf{k}, z, t) &= \int d\rho \int_0^\infty dz' \exp[i\mathbf{k}_\parallel \cdot \rho + k_\perp(z' - z)] \\ &\quad \times G(\rho, z', z, t).\end{aligned}\quad (30b)$$

In both Eqs. (29b) and (30b), we have made use of the translational invariance in the direction parallel to the surface. Note that, in our definition  $G_\parallel(\rho_1 - \rho_2, z, t) = G(\rho_1 - \rho_2, z, z, t)$ . In analogy with Eq. (28), the surface excess of the time-dependent scattering intensity of the system then is

$$S_s(\mathbf{k}, t) = \int_0^\infty dz [S(\mathbf{k}, z, t) - S_b(\mathbf{k}, t)], \quad (31)$$

where  $S_b(\mathbf{k}, t)$  is the scattering intensity observed in a spinodal decomposition experiment in the bulk.

In studies of spinodal decomposition one usually defines length scales from the decay of the real-space correlation function or by taking reduced moments of the momentum-space structure factor [21]. In this paper, we define the characteristic length  $l_\parallel(z, t)$  describing the growth of correlations in the parallel direction at a distance  $z$  from the surface as the distance over which the appropriate real-space correlation function decays to half its maximum value. Thus, in two-dimensional space,

$$G_\parallel(l_\parallel(z, t), z, t) = G_\parallel(0, z, t) / 2, \quad (32a)$$

while alternative definitions based on the structure factor would be (in general dimensions)

$$l_{\parallel}^{(1)}(z,t) = \int d\mathbf{k}_{\parallel} S_{\parallel}(\mathbf{k}_{\parallel}, z, t) / \int d\mathbf{k}_{\parallel} k_{\parallel} S_{\parallel}(\mathbf{k}_{\parallel}, z, t) \quad (32b)$$

or

$$l_{\parallel}^{(2)}(z,t) = \left[ \frac{\int d\mathbf{k}_{\parallel} S_{\parallel}(k_{\parallel}, z, t)}{\int d\mathbf{k}_{\parallel} (k_{\parallel})^2 S_{\parallel}(k_{\parallel}, z, t)} \right]^{1/2}. \quad (32c)$$

Note that the integrals over momentum need to be cut off at large  $\mathbf{k}$  in order to eliminate background structure due to uninteresting local correlations, which describe structure inside the growing domains rather than their size distribution. This problem does not occur for the definition in Eq. (32a) which is also easier to implement in the context of our numerical calculations and thus used throughout here. Of course, a perpendicular length scale  $l_{\perp}(z,t)$  can be defined similarly. In two-dimensional space, we use

$$G(0, z, z + l_{\perp}(z,t), t) = G(0, z, z, t) / 2. \quad (33)$$

For  $z \rightarrow \infty$ , these scales  $l_{\parallel}(z,t)$  and  $l_{\perp}(z,t)$  should tend smoothly towards the length scales that one uses to characterize spinodal decomposition in the bulk, which we denote simply as  $l_b(t)$ .

A particularly interesting feature of the late stages of spinodal decomposition in the bulk is the dynamic scaling property [21–23, 42, 58] of the correlation function, viz.,

$$G_b(\mathbf{r}, t) \equiv \tilde{G}_b\{r/l_b(t)\}, \quad (34a)$$

where  $\tilde{G}_b(\zeta)$  is a universal function. The corresponding statement for the structure factor in momentum space is

$$S_b(\mathbf{k}, t) = [l_b(t)]^d \tilde{S}_b\{kl_b(t)\}, \quad (34b)$$

where  $d$  is the dimensionality and  $\tilde{S}_b(\zeta)$  is a universal function. It is now well accepted that the characteristic length scale  $l_b(t)$  in the scaling regime increases according to a power law as

$$l_b(t) \propto t^{a_b}, \quad t \rightarrow \infty \quad (35)$$

with  $a_b = \frac{1}{3}$  for solid mixtures [22, 23]. This is referred to as the Lifshitz-Slyozov law [59], though this may be somewhat misleading because the original derivation of Lifshitz and Slyozov was in the context of binary mixtures where one of the phases is present in a vanishingly small fraction.

We hence make a similar scaling hypothesis with respect to parallel correlations near a surface, namely,

$$G_{\parallel}(\rho, z, t) = \tilde{G}_{\parallel}\{\rho/l_{\parallel}(z,t)\}, \quad (36a)$$

$$S_{\parallel}(\mathbf{k}_{\parallel}, z, t) = [l_{\parallel}(z,t)]^{d-1} \tilde{S}_{\parallel}\{k_{\parallel}l_{\parallel}(z,t)\}. \quad (36b)$$

Again we expect a power law

$$l_{\parallel}(z,t) \propto t^{a_{\parallel}}, \quad t \rightarrow \infty. \quad (37)$$

In Eqs. (36a), (36b), and (37), we have assumed the simple special case that there is a certain ‘‘universality,’’ i.e., we anticipate that neither the exponent  $a_{\parallel}$  nor the scaling functions  $\tilde{G}_{\parallel}, \tilde{S}_{\parallel}$  depend explicitly on the distance  $z$  from the wall. This assumption is plausible since the scaling

property of Eqs. (36a) and (36b) is expected only for such late times where

$$l_{\perp}(z,t) \gg z \quad (38)$$

and then the scattering behaves qualitatively in the same way as if it came right from the surface region ( $z=0$ ). Thus the only fashion in which  $l_{\parallel}(z,t)$  in Eq. (37) may depend on  $z$  is via a possible  $z$  dependence of the amplitude factor. Conversely, if we consider such a large value of  $z$  that the inverse of Eq. (38) holds [namely,  $l_{\perp}(z,t) \ll z$ ], then we simply expect that Eqs. (36a) and (36b) hold but with  $l_{\parallel}(z,t) = l_b(t)$ , because then the limiting boundary at  $z=0$  is not yet physically felt at a distance  $z$ .

As emphasized in part A of this section, the boundary conditions at  $z=0$  may be such that the equilibrium for one of the coexisting phases that form in the spinodal decomposition process may require the surface to be coated with a wetting layer (or drying layer, respectively). Since the initial condition of the surface usually will not contain such a layer, we have also to consider the dynamics of the formation of wetting layers [25, 31] as a competitive process to spinodal decomposition. In general, one also writes for the thickness of the growing wetting layer  $l_w(t)$  at late times a power law

$$l_w(t) \propto t^{a_w}, \quad t \rightarrow \infty. \quad (39)$$

However, we readily note that for short-range surface forces

$$a_w = 0, \quad (40)$$

i.e., a logarithmic growth law is expected [25–28].

### C. Surface effects in the framework of a linearized theory of spinodal decomposition

As is well known, a linearized theory of spinodal decomposition in the bulk [21, 22, 24] is obtained from Eq. (13) by expanding the nonlinear term around the average value  $\phi_0$  of the order parameter as  $\phi^3 \approx \phi_0^3 + 3\phi_0^2\delta\phi$ , which yields

$$\frac{\partial}{\partial \tau} \delta\phi(\mathbf{R}, \mathbf{Z}, \tau) = -\nabla^2(1 - 3\phi_0^2 + \frac{1}{2}\nabla^2)\delta\phi(\mathbf{R}, \mathbf{Z}, \tau), \quad (41)$$

where we continue to work in the dimensionless variables, for convenience. Fourier transformation then yields for the Fourier components  $\delta\phi_k(\tau)$  of  $\delta\phi(\mathbf{R}, \mathbf{Z}, \tau)$

$$\frac{\partial}{\partial \tau} \delta\phi_k(\tau) = k^2(1 - 3\phi_0^2 - \frac{1}{2}k^2)\delta\phi_k(\tau), \quad (42)$$

leading to the well-known exponential growth of long wavelength fluctuations,

$$\delta\phi_k(\tau) = \delta\phi_k(0) \exp[k^2(1 - 3\phi_0^2 - \frac{1}{2}k^2)\tau]. \quad (43)$$

Equation (42) shows that all fluctuations in the following range get exponentially amplified:

$$0 < k < k_c, \quad k_c = \sqrt{2 - 6\phi_0^2}; \quad (44)$$

and the maximum growth rate occurs at a wavelength  $\lambda_m$  given by

$$\lambda_m = \frac{2\pi}{k_m} = \frac{2\pi\sqrt{2}}{k_c} = 2\pi/\sqrt{1-3\phi_0^2}. \quad (45)$$

It is interesting to ask how the bulk behavior described by Eq. (43) is modified by the presence of a surface.

For an initial condition at an arbitrary temperature  $T > T_c$ , we have to confine ourselves to the experimentally important situation of a critical quench ( $\phi_0=0$ ) at  $\tau=0$  and assume that the surface field  $h_1$  is also switched on at a time  $\tau=0$ . For off-critical quenches, we would have to consider the growth of fluctuations around an inhomogeneous initial condition. This is because, for  $h_1=0$ , the counterpart of Eq. (13) for  $T > T_c$  with the boundary conditions as in Eqs. (14) and (15) does not admit a homogeneous off-critical solution. Similarly, if one considers the surface field to be present for all times, there is again no homogeneous solution for a system at critical composition with  $T > T_c$  and we would once again have to consider the growth of fluctuations (after the quench) around an inhomogeneous initial condition. In principle, this can be done but we do not wish to un-

duly complicate our analysis here. Note that one can also interpret our choice as a quench from infinite temperature ( $T \rightarrow \infty$ ) as initial condition, and then an arbitrary order parameter  $\phi_0$  can be chosen.

Equation (41) still holds for early times but is now complemented by the boundary conditions at the surface. Since the translational invariance of the system in the  $Z$  direction is broken, individual Fourier components such as those in Eq. (43) obviously do not satisfy the boundary conditions, Eqs. (14) and (15).

In order to make progress it is necessary to treat the coordinates  $\mathbf{R}, Z$  differently, writing  $\nabla^2 = \nabla_{\mathbf{R}}^2 + \partial^2/\partial Z^2$ , and from the start carrying out a Fourier transform with respect to  $\mathbf{R}$  only. Equation (41) then becomes

$$\frac{\partial}{\partial \tau} \delta\phi_{k_{\parallel}}(\mathbf{Z}, \tau) = \left[ k_{\parallel}^2 - \frac{\partial^2}{\partial Z^2} \right] \left[ 1 - 3\phi_0^2 - \frac{1}{2}k_{\parallel}^2 + \frac{1}{2}\frac{\partial^2}{\partial Z^2} \right] \times \delta\phi_{k_{\parallel}}(\mathbf{Z}, \tau). \quad (46)$$

This partial differential equation now has to be solved subject to the boundary conditions resulting from Eqs. (14) and (15), where we introduce analogous Fourier transforms and neglect nonlinear terms,

$$\left. \frac{\partial}{\partial \tau} \delta\phi_{k_{\parallel}}(\mathbf{Z}, \tau) = h_1 + g\delta\phi_{k_{\parallel}}(Z=0, \tau) + \gamma \frac{\partial}{\partial Z} \delta\phi_{k_{\parallel}}(\mathbf{Z}, \tau) \right|_{Z=0} - \left[ \frac{\gamma}{4} \right]^{2/3} \left. \frac{\partial^2}{\partial Z^2} \delta\phi_{k_{\parallel}}(\mathbf{Z}, \tau) \right|_{Z=0} - \frac{5}{6} \left[ \frac{\gamma}{4} \right]^{1/3} \left. \frac{\partial^3}{\partial Z^3} \delta\phi_{k_{\parallel}}(\mathbf{Z}, \tau) \right|_{Z=0}, \quad (47)$$

and

$$\left. \frac{\partial}{\partial Z} \left[ \delta\phi_{k_{\parallel}}(\mathbf{Z}, \tau) - 3\phi_0^2 \delta\phi_{k_{\parallel}}(\mathbf{Z}, \tau) + \frac{1}{2} \left[ k_{\parallel}^2 - \frac{\partial^2}{\partial Z^2} \right] \delta\phi_{k_{\parallel}}(\mathbf{Z}, \tau) \right] \right|_{Z=0} = 0. \quad (48)$$

Equations (46)–(48) thus extend the Cahn-Hilliard [24] linearized theory of spinodal decomposition to incorporate the effects of a free surface. For  $k_{\parallel}=0$  this set of equations is essentially equivalent to the description of Binder and Frisch [34] for the dynamics of surface enrichment in mixtures (apart from the fact that these authors considered only  $T > T_c$  and hence there deviations from equilibrium decay and one then does not have an exponential growth of fluctuations). It was found that in this case [34] the order parameter at the surface  $\delta\phi_{k_{\parallel}=0}(Z=0, \tau)$  reaches its equilibrium value much faster than the order parameter profile  $\delta\phi_{k_{\parallel}=0}(Z, \tau)$  at large distances  $Z$  from the surface.

The aim is to find a solution of Eqs. (46)–(48) that leads to Eq. (43), with  $k = k_{\parallel}$ , for  $Z = \infty$ , while for  $Z \rightarrow 0$  the boundary conditions enforce a relaxation governed by the surface terms and the parameters  $h_1$ ,  $g$ , and  $\gamma$ . Particularly interesting is the case  $k_{\parallel}=0$ , for which there is

no growth of waves in the bulk, while there is still relaxation near the surface. Since already for  $T > T_c$  the order parameter profile  $\delta\phi_{k_{\parallel}=0}(Z, \tau)$  decays with increasing  $Z$  in a nonmonotonic way, due to the formation of a depletion zone at intermediate distances from which the surface excess enriched at the surface has been transported [36], we expect an oscillatory decay of  $\delta\phi_{k_{\parallel}=0}(Z, \tau)$  to zero as  $Z \rightarrow \infty$  for  $T < T_c$  as well. This expectation is compatible with the numerical results (see below), where such a profile with oscillations that get damped out as  $Z$  increases is actually observed even for very early stages of surface-directed spinodal decomposition.

Since the analytic construction of  $\delta\phi_{k_{\parallel}=0}(Z, \tau)$  turns out to be rather difficult even for  $T > T_c$  [34], we do not attempt to compute  $\delta\phi_{k_{\parallel}}(Z, \tau)$  for  $T < T_c$  here. We only note, merely from dimensional analysis of Eq. (46), that the period of the damped oscillations in the  $Z$  direction should be given by the same length  $\lambda_m$  [Eq. (45)] that also controls the scale of the inhomogeneities formed in the bulk. Qualitatively, for a critical quench ( $\phi_0=0$ ) we expect to see a period of the damped oscillations of about  $2\pi$ . As we shall see below, this estimate is compatible with our numerical results.

Of course, it is well known that the linear theory of spinodal decomposition is quantitatively invalid, except if

one considers systems with large but finite range of interactions [65]. However, even for short-range systems where the nonlinear effects are important already in the initial stages of phase separation, numerical work [66] has shown that the linear theory underestimates the initial length scale (defined by the inverse of the structure factor peak position) by no more than 30%. Therefore the linear theory is useful at least as a rough guide to estimate the initial characteristic length scale of spinodal decomposition.

#### IV. NUMERICAL RESULTS

We now proceed to describe detailed numerical results obtained from discrete implementations of our model on two-dimensional (2D) lattices of size  $L_x \times L_z$ . We have implemented an Euler-discretized version of Eqs. (13)–(15) with an isotropically discretized Laplacian on 2D lattices with the boundary conditions of Eqs. (14) and (15) being implemented at  $Z=0$  (corresponding to the wall) and free boundary conditions at  $Z=L_z$ . Periodic boundary conditions are applied in the direction parallel to the surface, viz., the  $X$  direction. The mesh sizes of

our discretization are  $\Delta\tau=0.05$  and  $\Delta X=1.5$ . Before we proceed, some remarks about these mesh sizes are in order. First, the mesh sizes are too coarse to accurately mimic the solution of our original partial differential equation. Thus the discrete models we use should be understood in the spirit of cell-dynamical system (CDS) models, which provide a discrete space-time description that is dynamically equivalent to the continuum description [60]. Secondly, the mesh sizes are also too coarse to reproduce the precise behavior of the surface layer, as we will demonstrate shortly. However, the time scales of growth of the surface layer are much slower than the time scales of phase separation, if the parameters  $h_1, g, \gamma$  are chosen to be of order unity, as is physically reasonable. Effectively, the enriched layer at the surface only provides a preferential direction for the bulk to orient along. Thus our discrete space-time models, though not numerically accurate representations of the underlying partial differential short-range forces and spinodal decomposition in the bulk.

The numerical results presented below are for lattices with  $L_x=300$  and  $L_z=150$ . We have systematically checked for finite-size effects by both doubling and halv-

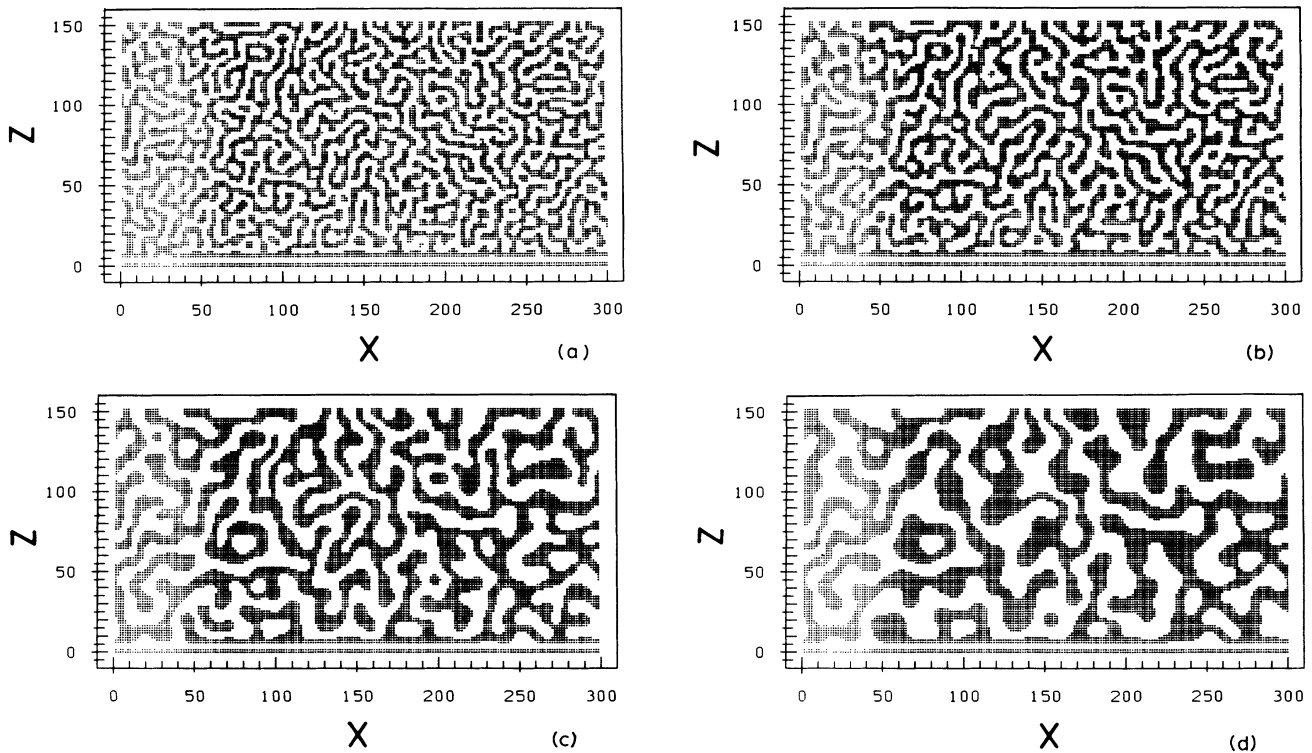


FIG. 3. Evolution pictures from our discrete implementation of the partial differential equation model with dynamical boundary conditions [Eqs. (13)–(15)] on a square lattice using Euler discretization with an isotropically discretized Laplacian. The discretization mesh sizes are  $\Delta\tau=0.05$  and  $\Delta X=1.5$  and our discrete model should be understood in terms of a cell-dynamical system (CDS) model which mimics the physics rather than the precise numerical solution of the partial differential equation. The lattice size is  $L_x \times L_z$  ( $L_x=300, L_z=150$ ) and the surface boundary conditions [Eqs. (14) and (15)] are applied at  $Z=0$ . Free boundary conditions are applied at  $Z=L_z$  and periodic boundary conditions are applied in the  $X$  direction. The parameter values are  $h_1=4$ ,  $g=-4$ , and  $\gamma=4$ , which correspond to a nonwet static equilibrium. The initial condition consists of uniformly distributed random fluctuations of amplitude  $\pm 0.025$  about a zero background, viz., a critical quench. Evolution pictures are shown for (a)  $\tau=50$ , (b)  $\tau=100$ , (c)  $\tau=500$ , and (d)  $\tau=4000$ .

ing the above sizes. On the time scales for which results are presented here (viz., dimensionless times of up to  $\tau=4000$ ), our results are unchanged if we increase the above sizes further. All averages for the calculation of correlation functions presented below are over 200 independent initial configurations, each of which consists of uniformly distributed random fluctuations of amplitude  $\pm 0.025$  about a zero background, viz., the so-called critical quench with an initial state at "infinite temperature."

First, we present results for the parameter values  $h_1=4$ ,  $g=-4$ , and  $\gamma=4$ . On the phase diagram of Fig. 2, these parameter values are seen to correspond to a nonwet static equilibrium. Figures 3(a)–3(d) show the temporal evolution of a typical disordered initial condition for these parameter values. Sites with positive order parameter (corresponding to species *A*) are marked by points whereas sites with negative order parameter (corresponding to species *B*) are left unmarked. The surface rapidly forms an enriched layer (in the preferred component *A*) followed by a depleted layer (due to the conservation law). This is followed by another enriched layer, which has about the same average thickness as the enriched layer adjacent to the wall, but is much more irregular locally. Further from the wall, the domain pattern has just the characteristic structure of bulk spinodal decomposition. The dynamics of phase separation in the vicinity of the surface is enhanced because of the orientational effect of the surface layer which preferentially aligns domains parallel to the surface. This results in an anisotropy of domain growth parallel and perpendicular to the surface, in the vicinity of the surface. The degree of anisotropy decreases with increasing  $Z$  and the bulk is (naturally) isotropic. An interesting feature is that the thickness of the two surface-enriched layers parallel to the wall increases much slower than the typical domain size in the bulk. Figure 4(a) shows the averaged profiles in the  $Z$  direction for the evolution pictures of Fig. 3. The averaged profiles are obtained by laterally averaging the order parameter profile  $\phi(X, Z, \tau)$  in the  $X$  direction (parallel to the surface) for a single run and then ensemble averaging over 50 different runs. In the surface region, one sees directed spinodal decomposition waves [19], which slowly propagate out into the bulk. Due to the averaging procedure we follow, the average profile decays to zero in the bulk.

As we have already remarked, the mesh sizes of our simulation are too coarse to precisely describe the dynamics of Eqs. (13)–(15) in regards to the growth of the surface-enriched layer. Figure 4(b) shows the laterally averaged profile from five runs for a 2D simulation of (13)–(15) on a lattice of the same size  $L_x=300$  and  $L_z=150$  but with a much finer mesh, viz.,  $\Delta\tau=0.001$  and  $\Delta X=0.4$ . It is clear from Fig. 4(b) that the surface-enriched layer has a somewhat larger growth than the profile of Fig. 4(a) would suggest. However, if we look at the location of the first zero of this profile  $R_1(\tau)$  as a function of time [Fig. 4(c)], it is clear that the growth of this surface layer is extremely slow for  $\tau > 1000$  and may be treated as being stationary on the time scales of interest for spinodal decomposition. In fact, since our state in equilibrium (see Fig. 2) corresponds to a nonwet phase

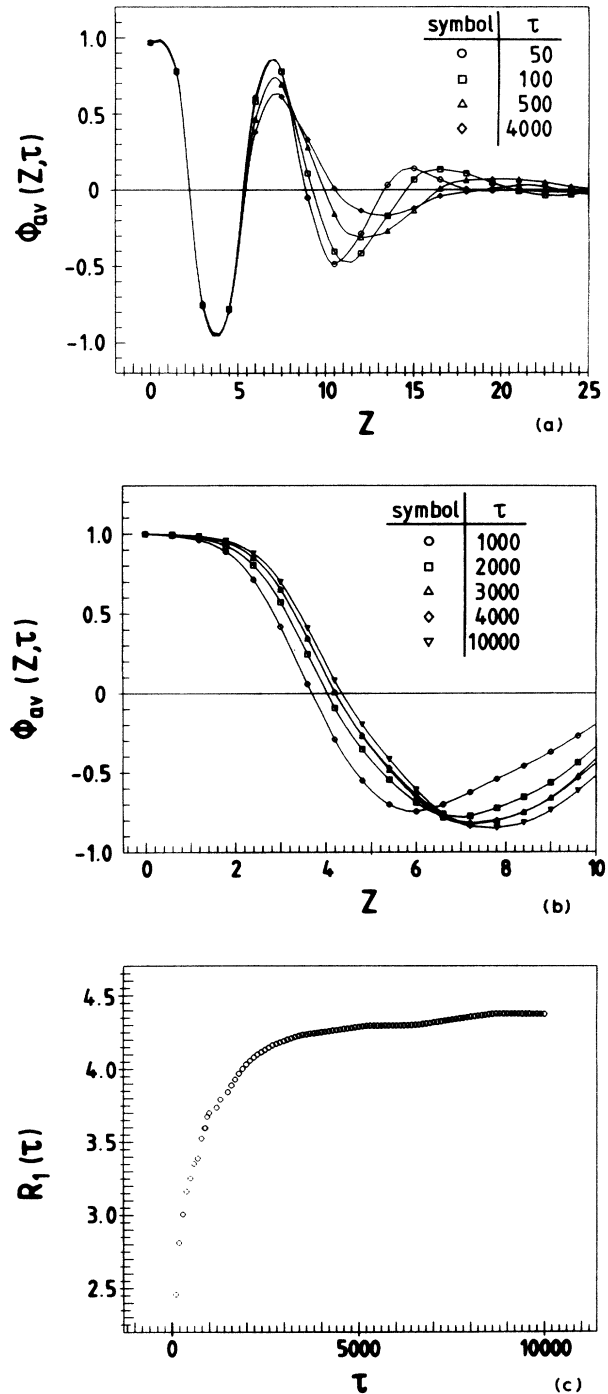


FIG. 4. (a) Averaged profiles for order parameter  $\phi_{av}(Z, \tau)$  as a function of  $Z$  (scaled distance from the surface) and  $\tau$  (scaled time) for our discrete model. The averaging is done laterally (in the direction parallel to the wall) and over an ensemble of 50 independent initial conditions. (b) Averaged profiles for order parameter  $\phi_{av}(Z, \tau)$  as a function of  $Z$  (scaled distance from the surface) and  $\tau$  (scaled time) for a fine mesh ( $\Delta\tau=0.001, \Delta X=0.4$ ) numerical implementation of the continuum model represented by Eqs. (13)–(15). (c) First zero crossing  $R_1(\tau)$  of the averaged profile of (b) as a function of time  $\tau$ . This measure of their thickness of the surface layer rapidly saturates out to its equilibrium value  $\sim 4.25$  dimensionless units and barely changes for  $\tau > 1000$ .

of the surface but is rather close to the wetting transition, we expect a surface-enriched layer of phase  $A$  at the surface which saturates at a thickness of several  $\xi_b$ ; thus the profile for  $\tau=10\,000$  in Fig. 4(b) may already be close to this final equilibrium enrichment layer. Clearly, the primary effect on the surface layer on the phase separation of the binary mixture, at least for the nonwet case considered here, is to provide a preferred direction. Our coarser discretization captures this feature and serves as a reasonable description of surface-affected spinodal decomposition. Naturally, one may expect that the case in which the surface is wet may not be appropriately described in terms of orientational effects. However, even in that case, as we demonstrate later, the growth of the enriched layer is so slow for short-ranged surface forces (logarithmic in time) that it does not interfere with phase separation (which is characterized by a power-law domain growth).

Figures 5(a)–5(d) show the correlation function parallel to the surface defined in Eq. (29a) as a function of the distance  $Z$  from the surface from very early times ( $\tau=10$ , where the linearized theory is valid) to times ( $\tau=4000$ ) deep into the asymptotic regime for spinodal decomposition in the bulk [60]. For purposes of comparison, we have also depicted the corresponding bulk correlation function as a solid line. At the surface ( $Z=0$ ), there is no correlation because the profile is already pinned to its equilibrium value and fluctuations are negligible. Also for  $Z=6$ , a distance comparable to the thickness of the surface-enriched layer [Fig. 4(b)], there is only a very weak shallow minimum; the correlation function for slightly smaller  $Z$  does not even show a minimum at all, but rather a monotonic decay. The general trend is that the correlation function for larger values of  $Z$  tends to the bulk correlation function, with the discrepancy between the bulk correlation function and the larger value

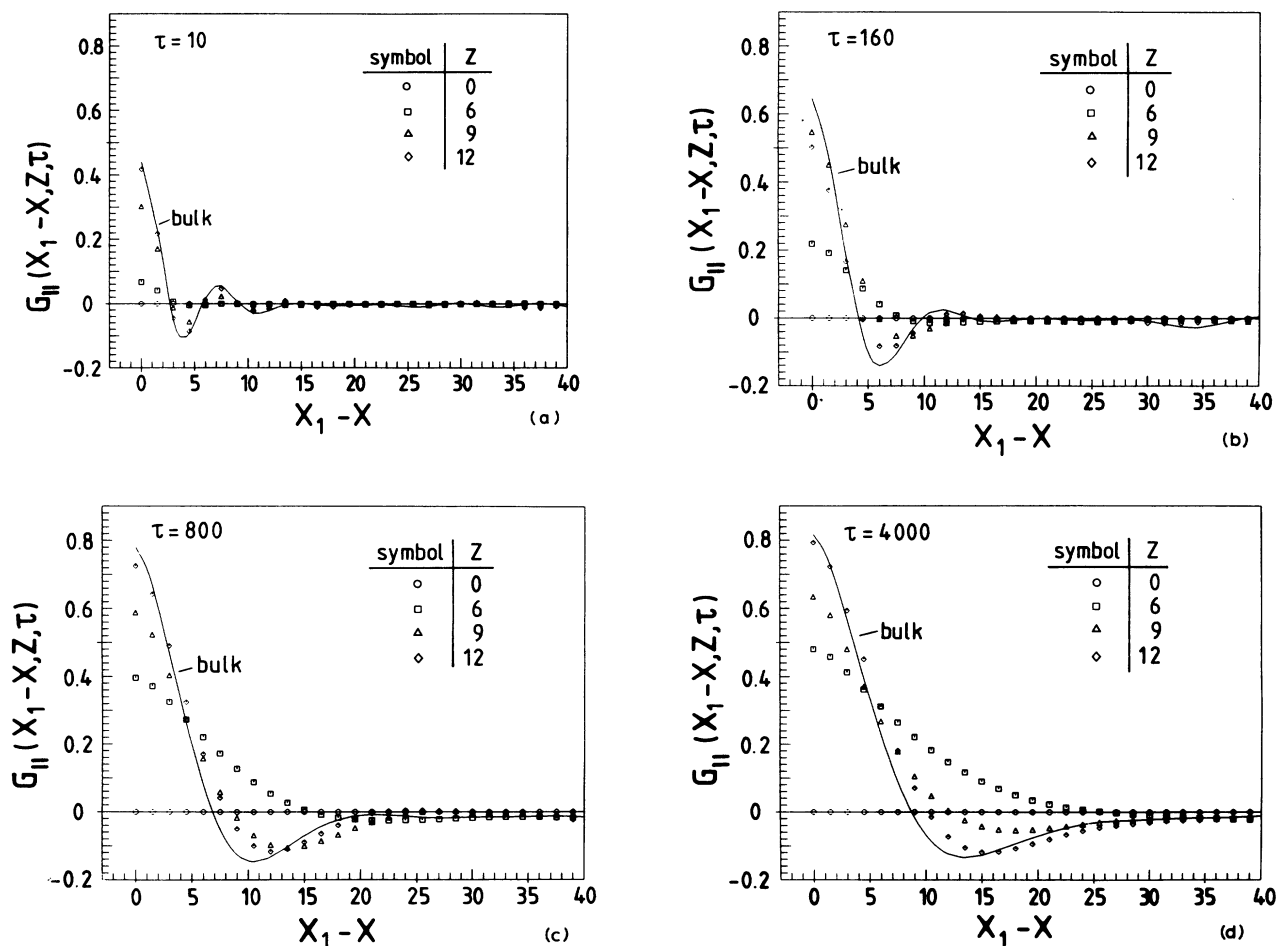


FIG. 5. Correlation functions in the direction parallel to the surface  $G_{||}(X_1 - X, Z, \tau)$  as a function of  $(X_1 - X)$  for different values of  $Z$  ( $=0, 6, 9, 12$ ) and  $\tau$  ( $=10, 160, 800, 4000$ ). The correlation functions are obtained as averages over 200 independent initial conditions and also an averaging over the variable  $X$  (using translational symmetry in the direction parallel to the surface). Each figure plots data for  $Z=0, 6, 9, 12$  (denoted by indicated symbols) and the bulk (denoted by a solid line). Data are for times (a)  $\tau=10$ , (b)  $\tau=160$ , (c)  $t=800$ , (d)  $t=4000$ .

of  $Z$  shown here ( $Z=12$ ) increasing with time, as the effect of the surface is felt deeper and deeper into the bulk. Figure 6 shows the characteristic size in the  $X$  direction as a function of distance from the surface  $Z$  and time  $\tau$ . As mentioned earlier, we define the characteristic domain size [denoted by  $l_{\parallel}(Z, \tau)$ ] as the distance in the  $X$  direction over which the correlation function in the  $X$  direction falls to half its maximum value [see Eq. (32a)]. Some cautionary remarks are in order at this stage regarding the precise interpretation of this length scale. In the surface region, as we demonstrate shortly, the correlation function does not exhibit good dynamical scaling, suggesting that there is more than one characteristic length scale in the vicinity of the surface. By virtue of its definition,  $l_{\parallel}(Z, \tau)$  is clearly a measure of the characteristic domain size in the  $X$  direction at any given time. But one should keep in mind that a plot of  $l_{\parallel}(Z, \tau)$  vs  $\tau$  in the vicinity of the surface would, in general, also contain the time dependence (albeit slow) of the nonuniversal scaling function. In spite of these qualifications, the data for the length scale  $l_{\parallel}(Z, \tau)$  appear to exhibit power-law domain growth in the intermediate to late stages of domain growth ( $\tau > 1600$ ). We have attempted to fit the data points for  $\tau > 1600$  to a power law of the form  $l_{\parallel}(Z, \tau) = A + B\tau^a$ . To get rid of the parameters  $A$  and  $B$ , we consider the function  $f(Z, \tau) = [l_{\parallel}(Z, \tau_2) - l_{\parallel}(Z, \tau)] / [l_{\parallel}(Z, \tau_2) - l_{\parallel}(Z, \tau_1)]$  where  $\tau_1 = 1600$  and  $\tau_2 = 4000$ , in this case. This new function depends on only one parameter  $a$  and we fit the data (consisting of

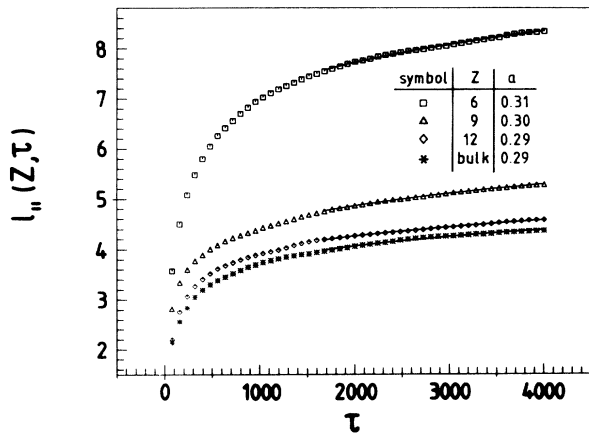


FIG. 6. Time dependence of length scales in the direction parallel to the surface [ $l_{\parallel}(Z, \tau)$ ] for  $Z=6, 9, 12$  (denoted by indicated symbols) and the bulk (denoted by \*). The length scales are defined as the distance at which the correlation function  $G_{\parallel}(X_1 - X, Z, \tau)$  falls to half its maximum value, viz.,  $G_{\parallel}(0, Z, t)$ . The data for  $\tau > 1600$  are fit to the power-law form  $l_{\parallel}(Z, \tau) = A + B\tau^a$  as described in the text and the resulting exponents are indicated in the figure. Error bars on the exponent values are  $\pm 0.02$ . The nonlinear fits are represented as solid lines superposed on the data points. As mentioned in the text, the length scale data obtained from one-dimensional correlation functions appear to somewhat underestimate the growth exponent for the bulk.

100 points) using a nonlinear fitting routine to determine  $a$ . The corresponding values (with error bars  $\pm 0.02$ ) are shown in Fig. 6 and the corresponding fits are depicted as solid lines on the sets of data points. We should point out that the structure factor data from one-dimensional (1D) data appear to underestimate the growth exponents

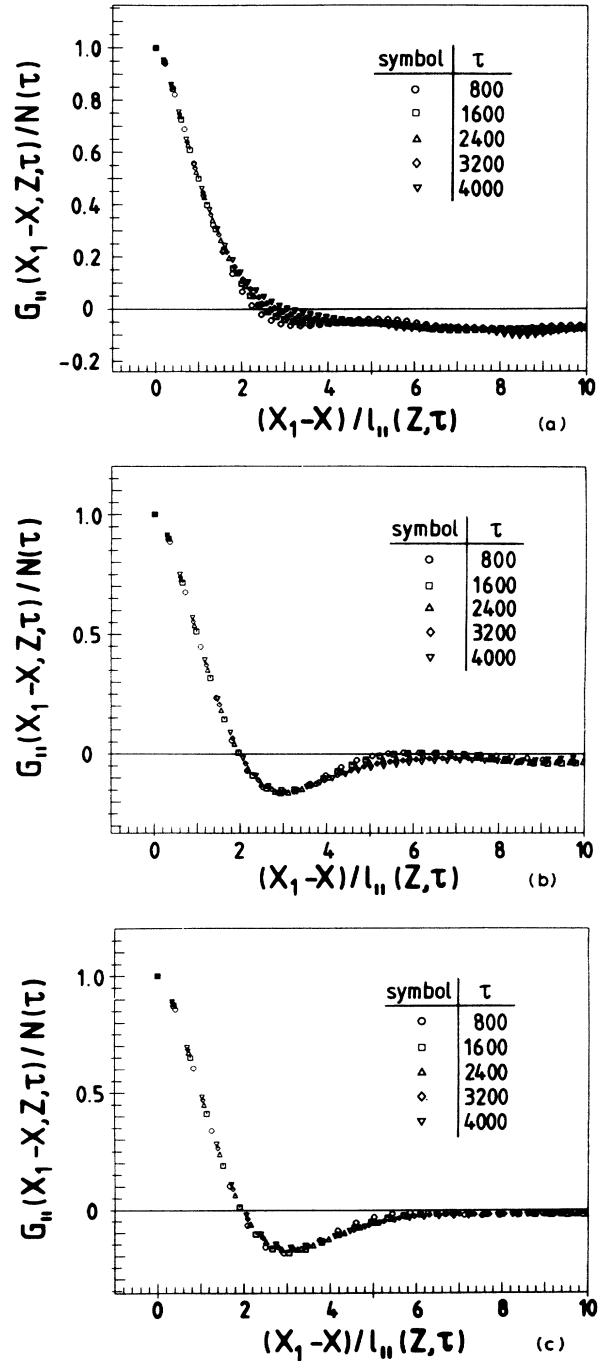


FIG. 7. Correlation functions from Fig. 5 normalized by maximum values [i.e.,  $G_{\parallel}(X_1 - X, Z, \tau) / N(\tau)$ , where  $N(\tau) = G_{\parallel}(0, Z, t)$ ] plotted as a function of the scaled variable  $(X_1 - X) / l_{\parallel}(Z, \tau)$  for times  $\tau=800, 1600, 2400, 3200, 4000$  (denoted by the symbols indicated). Different sets of data correspond to (a)  $Z=6$ ; (b)  $Z=12$ ; (c)  $Z=42$ .

somewhat. The data for bulk results have been obtained from 1D correlation functions for simulations with periodic boundary conditions in both directions, using the same kind of averaging procedure already described (with an additional averaging along the  $Z$  direction). The best fit to the data indicates an exponent  $a = 0.29 \pm 0.02$ , even though we know the bulk system to be already well into the scaling regime (characterized by  $a = \frac{1}{3}$ ) for the times indicated [60–61]. Given this fact, it appears that our data are consistent with a Lifshitz-Slyozov growth law, regardless of the value of  $Z$ . This is surprising, because, as we have pointed out before, the scaling function in the surface region is actually being slowly modulated in time. Thus the growth exponent is possibly more universal than the morphology of the growing patterns. This is not a novel idea, of course, and is implicit in the extension of Lifshitz-Slyozov ideas (proposed in the context of a far off-critical quench where isolated droplets grow) to the case of spinodal decomposition for critical quenches (where the morphology of interconnected

domains is very different from that in the far off-critical quenches) [62]. Of course, the slight enhancement of  $a$  for small  $Z$  should not be taken seriously, we rather expect that this reflects an enhancement of the amplitude  $B(Z)$  as  $Z \rightarrow 0$ .

Figures 7(a)–7(c) demonstrate the scaling function for times ranging from  $\tau = 800$  to 4000 and three different values of  $Z$ . In these figures, we have plotted,  $G_{\parallel}(X_1 - X, Z, \tau) \equiv G(X_1 - X, Z, \tau)$  normalized by its maximum value  $G_{\parallel}(0, Z, \tau) [=N(\tau)]$  vs  $(X_1 - X)/l_{\parallel}(Z, \tau)$ . Figure 7(a) depicts data for  $Z = 6$  and shows there is no dynamical scaling in the surface region with a slow upward trend of the scaling function. Figure 7(b) shows data for  $Z = 12$ , where the domain growth is almost identical to that for the bulk. Here, the scaling is much better but appears to break down at larger distances. Finally, Fig. 5(c) shows data for  $Z = 42$ , where the surface effects are not seen for the available times and the data exhibit good dynamical scaling as in the bulk. The slight deviation of the data for  $\tau = 800$  represents

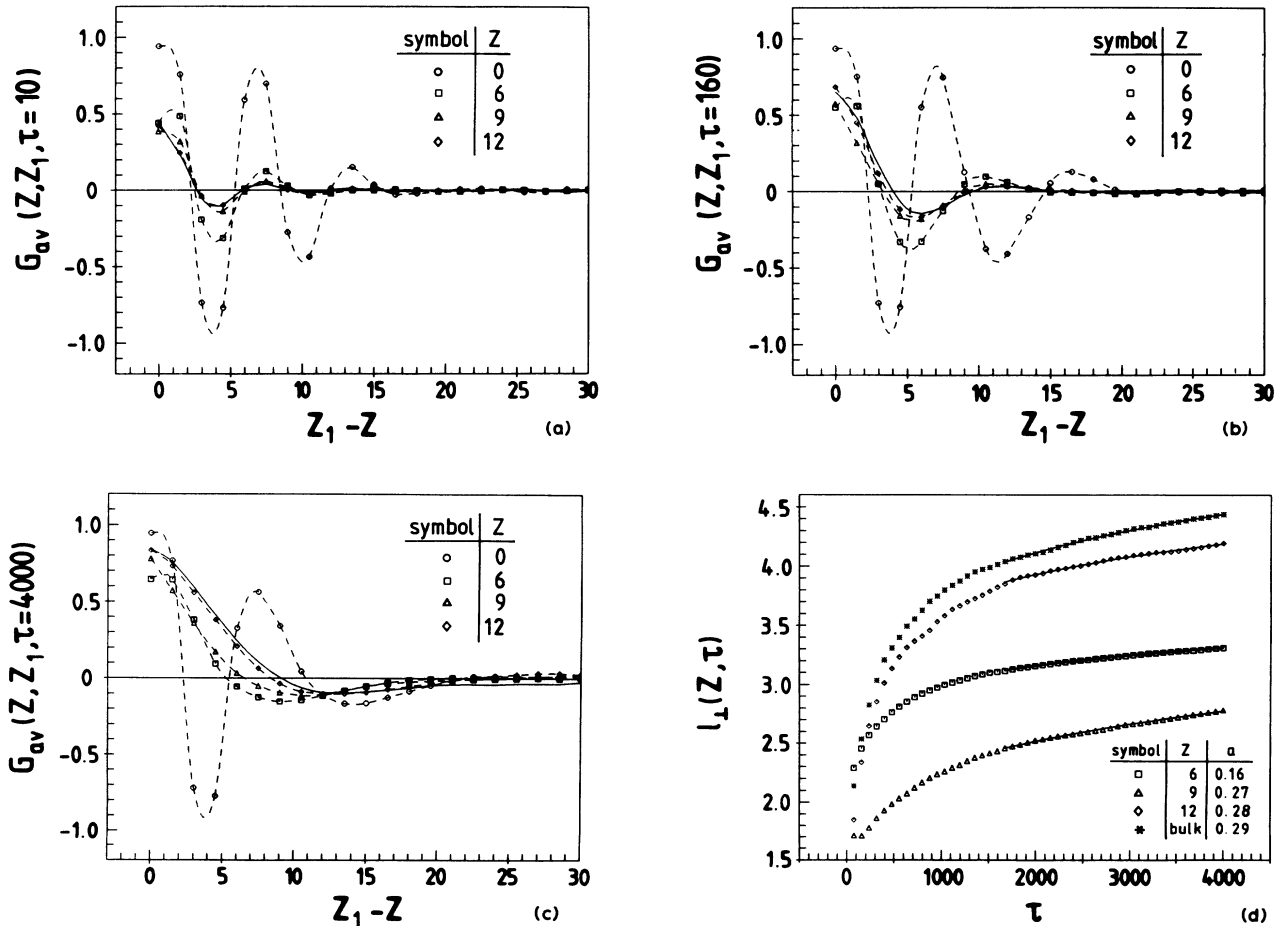


FIG. 8. Laterally averaged correlation functions  $G_{av}(Z, Z_1, \tau)$  as a function of  $(Z_1 - Z)$  from early to late times. Each figure plots data for  $Z = 0, 6, 9, 12$  (denoted by indicated symbols) and the bulk (denoted by a solid line). We have put dashed lines through the data to serve as guides to the eye. Data are shown for times (a)  $\tau = 10$ ; (b)  $\tau = 160$ ; (c)  $\tau = 800$ ; and (d)  $\tau = 4000$ .

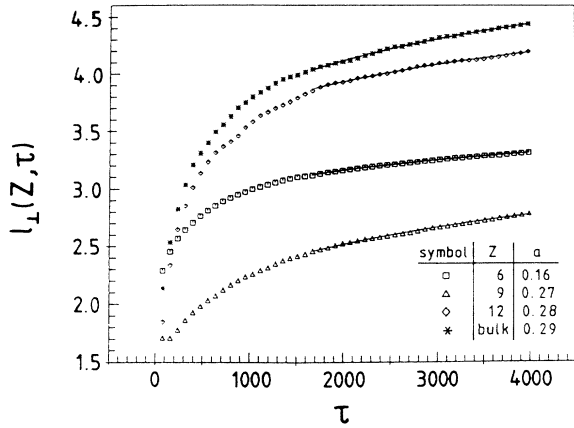


FIG. 9. Average length scales in the  $Z$  direction  $l_1(Z, \tau)$  as a function of  $Z$  and  $\tau$ . The length scale  $l_1(Z, \tau)$  is defined as the distance over which  $G_{av}(Z, Z_1, \tau)$  falls to half its maximum value. Data for different values of  $Z$  are denoted by the indicated symbols and the best-fit exponents (for  $\tau > 1600$ ) for a power-law growth are indicated alongside. The best-fit curves for  $\tau > 1600$  are plotted as solid lines superposed on the data sets.

corrections to dynamic scaling, as are well known from corresponding simulations of spinodal decomposition in the bulk.

Figures 8(a)–8(c) show data for the laterally averaged (i.e., in the  $X$  direction) correlation function [which we denote as  $G_{av}(Z, Z_1, \tau) \equiv G(0, Z, Z_1, \tau)$ ] as a function of

$Z_1 - Z$  from early to late times. Because of the breaking of translational symmetry by the surface, the correlation function depends on both  $Z_1$  and  $Z$ , until one is deep into the bulk. We have plotted dashed lines through the correlation function data for different values of  $Z$  to serve as guides to the eye. Furthermore, we have also plotted the corresponding bulk data as a solid line, for purposes of comparison. The data for  $Z = 0$  are directly correlated with the averaged profiles we presented in Fig. 4(a). For the correlation functions in the  $Z$  direction, we observe that the data for  $Z = 12$  are already very close to the bulk form, unlike in the  $X$  direction. We can also define length scales in the  $Z$  direction as the distance over which the correlation function  $G_{av}(Z, Z_1, \tau)$  falls to half its maximum value [see Eq. (33)]. However, these length scales should be carefully interpreted as being averaged lengths along the  $Z$  direction, because the length scale actually varies continuously as a function of  $Z$ . Figure 9 shows the length scale  $l_1(Z, \tau)$  as a function of time  $\tau$ . We have used the same fitting procedure as described previously to fit the data for  $\tau > 1600$  to a power-law form. In this case, the data for  $Z = 6$  (near the surface) exhibit an exponent of  $a = 0.16 \pm 0.02$ . This is considerably slower than the growth for other values of  $Z$ , which again appears to be consistent with Lifshitz-Slyozov growth. The low value for small  $Z$  is simply a kind of crossover, since the correlation function  $G_{av}(Z, Z_1, \tau)$  then also reflects the finite length scale of the surface enrichment layer, as discussed above.

We next present results for the parameter values

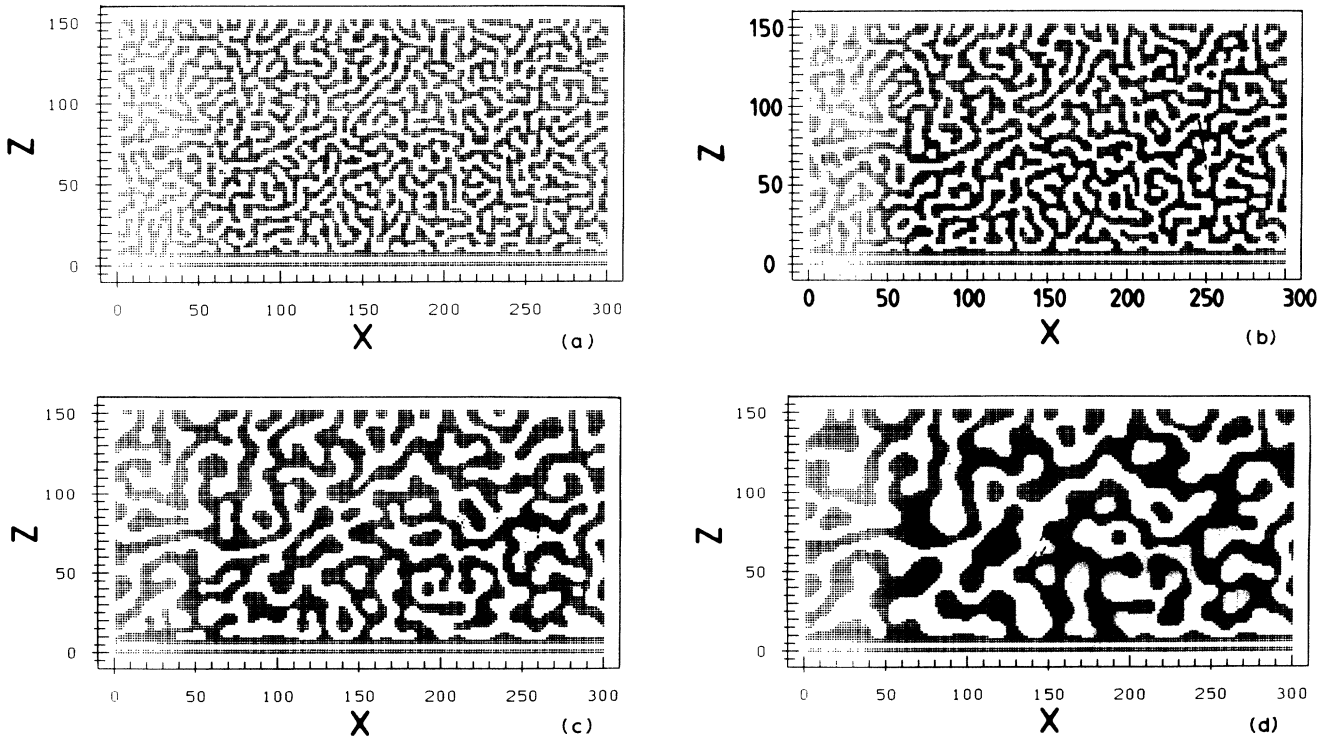


FIG. 10. Evolution pictures of our discrete implementation, analogous to Fig. 3, but for parameter values  $h_1 = 8$ ,  $g = -4$ , and  $\gamma = 4$ , which correspond to a wet static equilibrium for the underlying continuum model (marked by a  $\times$  in Fig. 2).

$h_1=8$ ,  $g=-4$ , and  $\gamma=4$ . These parameter values correspond to a wet static equilibrium (see Fig. 2). However, at the outset, we should caution the reader that the wetting transition does not appear to interfere seriously with the behaviors already seen for  $h_1=4$  (the nonwet case). This is because, in our model with short-ranged surface fields, the wetting layer grows out logarithmically in time and, to a good approximation, is again stationary on the time scales of phase separation. Thus, as previously, we are justified in using a coarse discretization mesh as the primary influence of the surface layer is orientational rather than dynamical.

Figure 10 shows evolution pictures from our discrete implementation of Eqs. (13)–(15). Again, the surface gets rapidly enriched in the preferred component  $A$  (marked by points) and this is followed by a depletion layer which is rich in  $B$  (not marked) and a second (more irregular) enrichment layer in  $A$ . These snapshot pictures do not look very different from their counterparts in the nonwet case, described in Fig. 3. Figure 11(a) shows the laterally and ensemble averaged profiles  $\phi_{av}(Z, \tau)$  as a function of  $Z$  for times  $\tau=50, 100, 500$ , and  $4000$ . As before, our coarse discretization does not capture the precise dynamical behavior of the interface. We demonstrate this in Fig. 11(b), which shows results for the laterally and ensemble averaged order parameter  $\phi_{av}(Z, \tau)$  for five runs with a  $300 \times 150$  lattice and much finer mesh sizes  $\Delta\tau=0.001$  and  $\Delta X=0.4$ . However, for the dynamics of spinodal decomposition adjacent to the layer, this is not a relevant quantity. Figure 11(c) shows the corresponding growth for the first zero crossing  $R_1(\tau)$  of the laterally averaged profile of Fig. 11(b) and is again seen to change rather slowly in time. While Fig. 11(a) looks like its nonwet counterpart [Fig. 4(a)], the finer scale [Fig. 11(b)] reveals characteristic distinctions from the nonwet case [Fig. 4(b)]: right at the surface the order parameter is strongly enhanced over its bulk value ( $\phi=1$  in our normalization), and the profile decays in two steps—on a scale  $Z \sim 1$  to  $\phi=1$  and on a larger scale  $l_w(\tau)$  an interface between the wetting layer and a depletion layer with  $\phi \cong -1$  occurs. For  $\tau \rightarrow \infty$ , we expect a logarithmic divergence of  $l_w(\tau)$  [25–28].

Figures 12(a)–12(d) show the correlation function in the  $X$  direction (parallel to the wall) for different values of  $Z$ . As one might expect, these are qualitatively similar to those of the previous case, with the only difference being that the effects of the surface are more marked—a consequence of a more enriched layer at the surface than in the previous case. Figure 13 shows the length scales in the  $X$  direction,  $l_{\parallel}(Z, \tau)$  as a function of  $\tau$ , for various values of  $Z$ . In general, the domain growth is a bit faster than in the nonwet case but the growth exponents are still consistent with Lifshitz-Slyozov growth, again reflecting a robust universality.

Plots of the normalized structure factors  $G_{\parallel}(X_1 - X, Z, \tau)/N(\tau)$  [where  $N(\tau) = G_{\parallel}(0, Z, \tau)$ ] versus the scaled distances  $(X_1 - X)/l_{\parallel}(Z, \tau)$  again are very similar to the nonwet case and hence not shown here. As previously, there is no clear dynamical scaling in the surface region and the dynamical scaling is not particularly good for  $Z=12$  either. Of course, dynamic scaling is

recovered deep into the bulk as  $Z=42$ . Under these circumstances (where  $Z$  is larger than the characteristic length scales) the scaling functions are practically indistinguishable from those in Fig. 7(c), which means that the

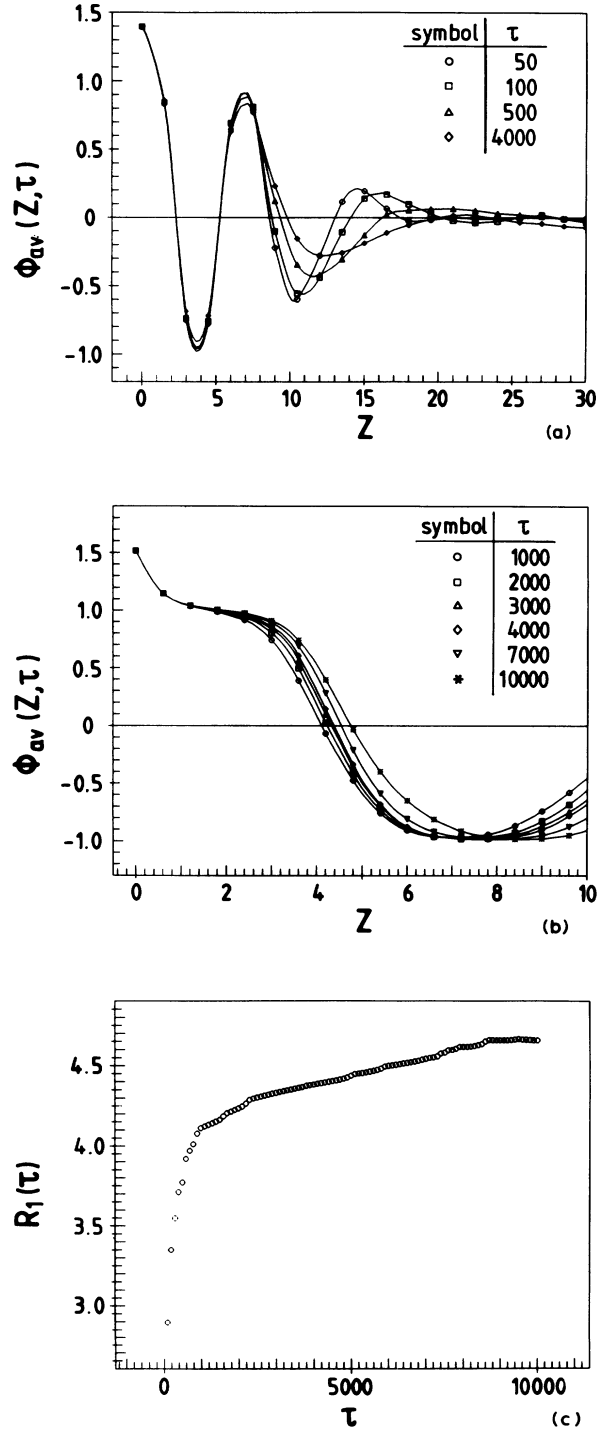


FIG. 11. Analogous to Figs. 4(a)–4(c) but for parameter values  $h_1=8$ ,  $g=-4$ , and  $\gamma=4$ , which correspond to a wet static equilibrium for the underlying continuum model.

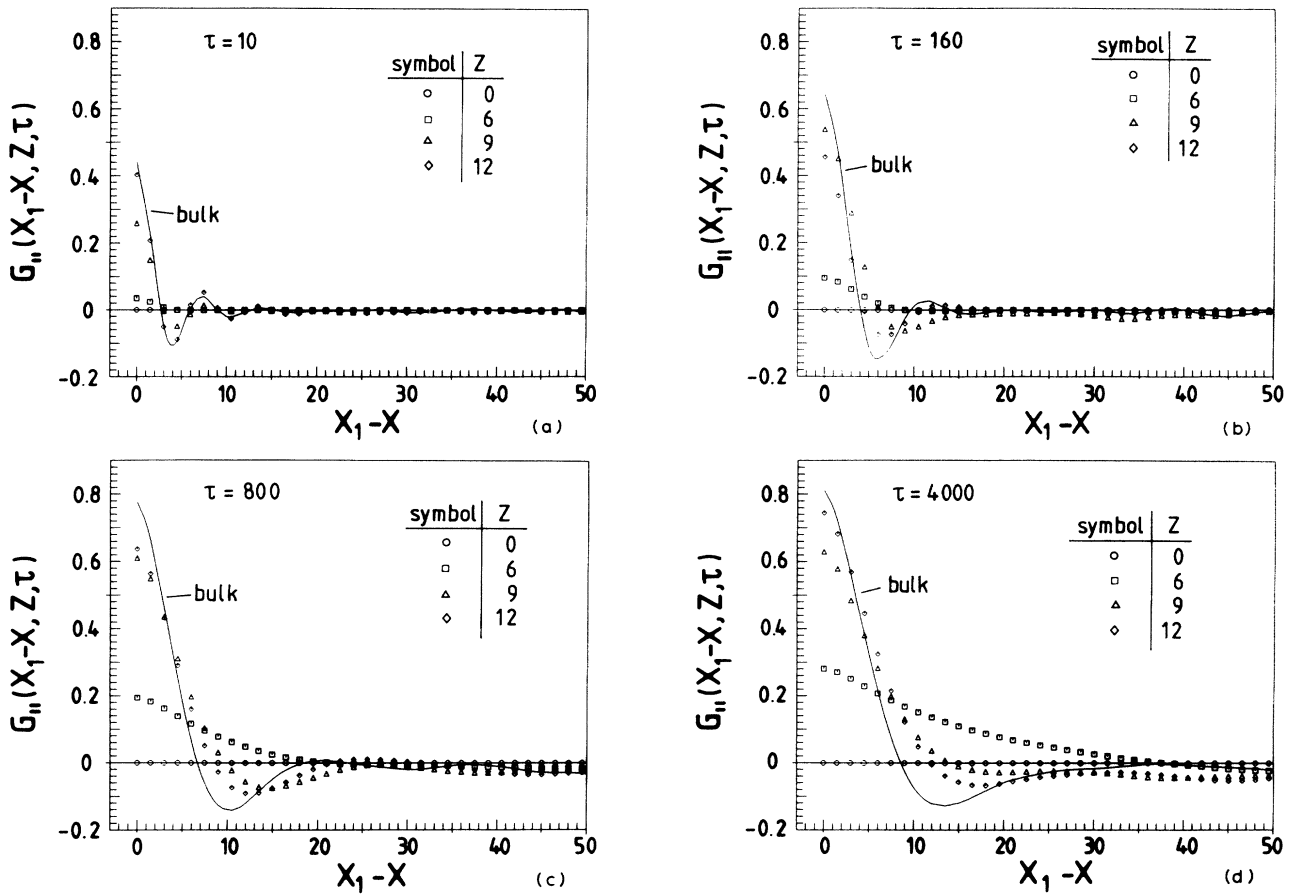


FIG 12. Analogous to Fig. 5, but for the parameter values  $h_1 = 8, g = -4,$  and  $\gamma = 4.$

different boundary conditions have no effect deep into the bulk.

Finally, Fig. 14 shows the average length scale in the perpendicular direction  $l_{\perp}(Z, \tau)$  as a function of time  $\tau$  for different values of  $Z$ . Apart from  $Z = 6$ , the other growth exponents appear to be consistent with the

Lifshitz-Slyozov growth law. The small value of the effective growth exponent  $a$  for  $Z = 6$  may be interpreted as a kind of weighted average between the growth exponent  $a_w$  of the wetting layer (logarithmic growth) and the Lifshitz-Slyozov exponent  $a = \frac{1}{3}$  that applies in the bulk.

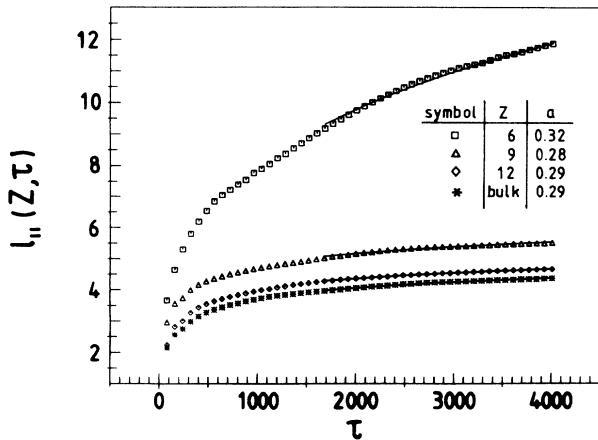


FIG. 13. Analogous to Fig. 6, but for the parameter values  $h_1 = 8, g = -4,$  and  $\gamma = 4.$

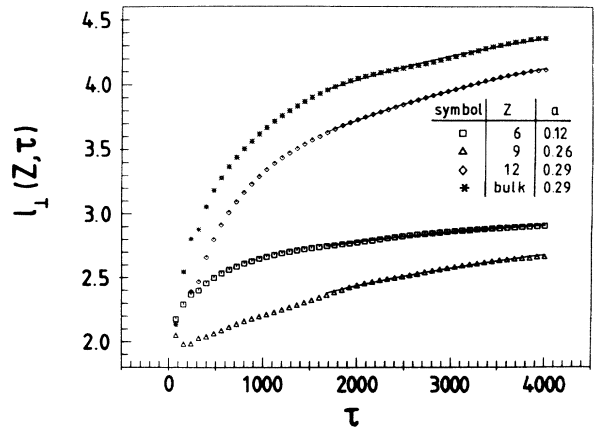


FIG. 14. Analogous to Fig. 9, but for the parameter values  $h_1 = 8, g = -4,$  and  $\gamma = 4.$

## V. SUMMARY AND DISCUSSION

In this paper, we have discussed decomposition in semi-infinite geometry, for the simplest possible case, i.e., where the kinetics is due to an interdiffusion of atoms via nearest-neighbor hopping events (in an Ising spin representation of a lattice model, this is the Kawasaki spin-exchange model, while in field-theoretic treatments of critical dynamics this is known as “model B”), and only short-range forces due to the surface are considered. We pay much attention to a proper use of the appropriate boundary conditions at the surface, and are thus able to distinguish cases where the surface in thermal equilibrium is nonwet from cases where it is wet.

Our study consists of two parts: in the first part, we formulate the general theoretical framework in which these phenomena should be described. By a suitable combination of ingredients from the theory of surface critical phenomena, wetting, and phase separation kinetics, we identify the general formalism that describes how structure factors and correlation functions near the surface differ from their counterparts in the bulk, and define length scales that can measure the anisotropy of the growth of phase-separated domains near the surface [ $l_{\parallel}(Z, \tau)$  and  $l_{\perp}(Z, \tau)$ , respectively]. Finally the exponential growth of fluctuations in the initial stages and the expected scaling behavior in the late stages are discussed qualitatively.

In the second part of our study, we present numerical results obtained from “computer experiments” using cell-dynamical system models to simulate “critical quenches” [i.e., only a bulk composition equal to the critical composition is considered,  $\phi_0=0$  in Eq. (46)]. We consider two different cases. In the first case the equilibrium state of the surface is nonwet, in the other case the surface is wet in equilibrium. The motivation for these choices is to see a possible effect of wetting phenomena on the dynamics of spinodal decomposition. We find, however, that the effect of these different boundary conditions at the surface is surprisingly minor: in both the wet and the nonwet case, an enrichment layer at the surface forms and very slowly grows in thickness. The only difference is that in the nonwet case the growth of the thickness of this layer basically stops at late times, while in the wet case the thickness continues to increase logarithmically in the time and the fine structure of the profile right at the surface is different [cf. the single-step profile Fig. 4(b) in contrast to the two-step profile, Fig. 11(b)]. Since the scale of inhomogeneities in phase separation grows according to the Lifshitz-Slyozov law [i.e.,  $l(\tau) \propto \tau^{1/3}$ ], the linear dimensions of the  $A$ -rich ( $B$ -rich) domains in the bulk at late times are much larger than any such surface-induced wetting layer, at least for the situation in which the surface forces are short ranged.

In both cases of wet or nonwet boundary conditions at the surface, the order parameter exhibits an oscillatory structure that rapidly decays to zero as one moves into the bulk. The reason for this observation is that both the formation of a surface enrichment layer and the formation of a true wetting layer require (from the condition

that the masses of both constituents  $A, B$  are conserved) the formation of an adjacent depletion zone of about the same thickness, where this excess concentration at the surface is being taken from. Therefore, at the surface, one full period of a concentration wave (with wave vector in  $Z$  direction) must form. Since in the bulk the local concentration (averaged along the  $X$  direction parallel to the surface) must be homogeneous in the  $Z$  direction, this wavelike oscillation at the surface must decay to zero as one progresses into the bulk. Alternatively, one can view the effect of the surface as an orientational bias on the forming domains: near the surface it is more likely to orient the (typically somewhat irregular and elongated) domains (rich in species of one kind) parallel to the surface rather than perpendicular to it. For this reason, the length scale  $l_{\parallel}(Z, \tau)$  for small  $Z$  is also numerically larger than the length scale  $l_b(\tau)$  in the bulk. Conversely, the length scale in perpendicular direction is a kind of weighted average which also includes a contribution from the much thinner wetting layer (or surface enrichment layer, respectively) and  $l_{\perp}(Z, \tau)$  is numerically smaller (for not too large  $Z$ ) than  $l_b(\tau)$ . In the fit to power laws this effect shows up in a slight increase of the exponent  $a_{\parallel}$  for small  $Z$  [and a distinct reduction of the exponent  $a_{\perp}$  describing the growth of  $l_{\perp}(Z, \tau)$ ]. However, we believe that this apparent change of exponents is simply a crossover phenomenon, and it is rather the amplitude in the power law for the characteristic lengths  $l_{\parallel}(Z, \tau)$ ,  $l_{\perp}(Z, \tau)$  that shows some  $Z$  dependence. It is rather natural to assume—though hard to prove numerically—that in our model all these lengths  $l_b(Z, \tau)$ ,  $l_{\parallel}(Z, \tau)$ , and  $l_{\perp}(Z, \tau)$  are described by the same growth exponent, i.e.,  $a = \frac{1}{3}$ .

While our study reveals again a rather good confirmation of dynamic scaling behavior in the bulk, for the time scales available in our study, in the region near the surface rather pronounced deviations have been found. We feel that this is a residual influence of the short length scale of the surface enrichment or wetting layer, that interferes with the growing length scale of bulk spinodal decomposition, just as this is responsible for the apparently changed effective growth exponents  $a_{\parallel}$  and  $a_{\perp}$ . If we were able to carry our simulations to much later times, one would presumably see a much better defined scaling, but this would require a huge numerical effort that does not seem to be possible.

Apart from this restriction, our study is only a first step towards a complete understanding in several respects. First, the effects of choosing off-critical concentrations ( $\phi_0 \neq 0$ ) should be investigated. Secondly, there is a need to investigate the effect of long-ranged surface effects, which are more realistic under most physical circumstances. Thirdly, and if one has an application to the experimentally crucial system of binary fluids in contact with a wall, the inclusion of hydrodynamic forces will be necessary. Finally, we note that most experimental studies of surface effects on spinodal decomposition do not study surfaces of bulk systems but rather a thin film geometry. Since the latter geometry is rather easily included in the framework of our theoretical modeling, we intend to report on such study in the near future [45].

## ACKNOWLEDGMENTS

S.P. expresses his gratitude to the Deutsche Forschungsgemeinschaft (DFG) for partial support under

Sonderforschungsbereich 262. S.P. is grateful to H. L. Frisch for a number of stimulating discussions and to A. Bray for some critical comments.

- 
- [1] *Fluid Interfacial Phenomena*, edited by C. A. Croxton (Wiley, New York, 1986).
- [2] J. Rowlinson and B. Widom, *Molecular Theory of Capillarity* (Oxford University Press, Oxford, 1982).
- [3] *Fundamentals of Inhomogeneous Fluids*, edited by D. Henderson (Dekker, New York, 1992).
- [4] K. Binder, in *Phase Transitions and Critical Phenomena*, edited by C. Domb and J. L. Lebowitz (Academic, London, 1983), Vol. 8, p. 1.
- [5] H. W. Diehl, in *Phase Transitions and Critical Phenomena*, edited by C. Domb and J. L. Lebowitz (Academic, London, 1986), Vol. 10, p. 75.
- [6] S. Dietrich, in *Phase Transitions and Critical Phenomena*, edited by C. Domb and J. L. Lebowitz (Academic, London, 1988), Vol. 12, p. 1.
- [7] P. G. de Gennes, *Rev. Mod. Phys.* **57**, 827 (1985).
- [8] D. E. Sullivan and M. M. Telo da Gama, in Ref. [1], p. 45.
- [9] E. H. Hauge, in *Fundamental Problems in Statistical Physics VI*, edited by E. G. D. Cohen (North-Holland, Amsterdam, 1985), p. 65.
- [10] M. E. Fisher, *J. Stat. Phys.* **34**, 667 (1984); *J. Chem. Soc. Faraday Trans.* **282**, 1569 (1986).
- [11] J. M. Blakely, in *Chemistry and Physics of Solids Surfaces*, edited by R. Vanselow (CRC, Boca Raton, FL, 1979), Vol. 2, p. 1.
- [12] H. Dosch, *Evanescence Scattering and Phase Transitions in Semi-Infinite Matter* (Springer, Berlin, 1991).
- [13] R. Lipowsky, *J. Appl. Phys.* **55**, 2485 (1984); *Ferroelectrics* **73**, 69 (1987).
- [14] J. F. Van der Veen, B. Pluis, and A. G. Denier van der Gon, in *Kinetics of Ordering and Growth at Surfaces*, edited by M. G. Lagally (Plenum, New York, 1990), p. 343.
- [15] B. Q. Shi, C. Harrison, and A. Cumming, *Phys. Rev. Lett.* **70**, 206 (1993).
- [16] H. Tanaka, *Phys. Rev. Lett.* **70**, 53 (1992).
- [17] P. Wiltzius and A. Cumming, *Phys. Rev. Lett.* **66**, 3000 (1991).
- [18] F. Bruder and R. Brenner, *Phys. Rev. Lett.* **69**, 624 (1992).
- [19] R. A. L. Jones, L. J. Norton, E. J. Kramers, F. S. Bates, and P. Wiltzius, *Phys. Rev. Lett.* **66**, 1326 (1991).
- [20] U. Steiner, E. Eiser, J. Klein, A. Budkowski, and L. J. Fetters, *Science* **258**, 1126 (1992).
- [21] J. D. Gunton, M. San Miguel, and P. S. Sahni, in *Phase Transitions and Critical Phenomena*, edited by C. Domb and J. L. Lebowitz (Academic, London, 1983), Vol. 8, p. 267.
- [22] K. Binder, in *Materials Science and Technology, Vol. 5: Phase Transformations in Materials*, edited by R. W. Cahn, P. Haasen, and E. J. Kramer (VCH, Weinheim, 1991), p. 405.
- [23] *Dynamics of Ordering Processes in Condensed Matter*, edited by S. Komura and H. Furukawa (Plenum, New York, 1988).
- [24] J. W. Cahn and J. E. Hilliard, *J. Chem. Phys.* **28**, 258 (1958); *J. W. Cahn, Acta Metall.* **9**, 795 (1961).
- [25] R. Lipowsky, *J. Phys. A* **18**, L585 (1985).
- [26] R. Lipowsky and D. A. Huse, *Phys. Rev. Lett.* **52**, 353 (1986).
- [27] I. Schmidt and K. Binder, *Z. Phys. B* **67**, 369 (1987).
- [28] K. K. Mon, K. Binder, and D. P. Landau, *Phys. Rev. B* **35**, 3683 (1987); *J. Appl. Phys.* **61**, 4409 (1987); K. Binder, in *Kinetics of Ordering and Growth at Surfaces*, edited by M. G. Lagally (Plenum, New York, 1990), p. 31.
- [29] M. Grant, *Phys. Rev. B* **37**, 5705 (1988).
- [30] R. Bausch and R. Blossey, *Europhys. Lett.* **14**, 125 (1991).
- [31] S. Puri and K. Binder, *Z. Phys. B* **86**, 263 (1992).
- [32] R. C. Ball and R. L. H. Essery, *J. Phys. Condens. Matter* **2**, 10303 (1990).
- [33] G. Brown and A. Chakrabarti, *Phys. Rev. A* **46**, 4829 (1992).
- [34] K. Binder and H. L. Frisch, *Z. Phys. B* **84**, 403 (1991).
- [35] K. Binder and H. L. Frisch, in *Dynamical Phenomena at Interfaces, Surfaces, and Membranes*, edited by D. Beysens, N. Boccara, and G. Forgacs (Nova Science, Commack, NY, 1992), p. 435.
- [36] S. Puri and K. Binder, *Phys. Rev. A* **46**, 4487 (1992); S. Puri and H. L. Frisch, *J. Chem. Phys.* **79**, 5560 (1993).
- [37] K. Kawasaki, in *Phase Transitions and Critical Phenomena*, edited by C. Domb and M. S. Green (Academic, London, 1972), Vol. 2, Chap. 11.
- [38] H. W. Diehl and H.-K. Janssen, *Phys. Rev. A* **45**, 7145 (1992).
- [39] P. C. Hohenberg and B. I. Halperin, *Rev. Mod. Phys.* **49**, 435 (1977).
- [40] K. Kawasaki and T. Ohta, *Prog. Theor. Phys.* **59**, 362 (1978).
- [41] E. Siggia, *Phys. Rev. A* **20**, 595 (1979).
- [42] H. Furukawa, *Adv. Phys.* **34**, 703 (1985).
- [43] H. Furukawa, *Physica A* **123**, 497 (1984).
- [44] T. Koga and K. Kawasaki, *Phys. Rev. A* **44**, 817 (1991); S. Puri and B. Dünweg, *ibid.* **45**, 6977 (1992); A. Shinozaki and Y. Oono, *Phys. Rev. E* **48**, 2612 (1993).
- [45] S. Puri and K. Binder, *J. Stat. Phys.* (to be published).
- [46] W. I. Goldberg, C. H. Shaw, J. S. Huang, and M. S. Piant, *J. Chem. Phys.* **68**, 484 (1978); Y. C. Chou and W. I. Goldberg, *Phys. Rev. A* **20**, 2105 (1979); **23**, 858 (1981); N. C. Wong and C. M. Knobler, *J. Chem. Phys.* **69**, 725 (1978); *Phys. Rev. A* **24**, 3205 (1981).
- [47] H. L. Snyder and P. Meakin, *J. Chem. Phys.* **79**, 5588 (1983).
- [48] T. Hashimoto, in *Materials Science and Technology, Vol. 12: Structure and Properties of Polymers*, edited by R. W. Cahn, P. Haasen, and E. J. Kramer (VCH, Weinheim, 1993).
- [49] J. D. Weeks, in *Ordering in Strongly Fluctuating Condensed Matter Systems*, edited by T. Riste (Plenum, New York, 1980), p. 293.
- [50] H. Van Beijeren and I. Nolden, in *Structure and Dynamics of Surfaces II*, edited by W. Schommers and P. Blanckenhagen (Springer, Berlin, 1987), p. 259.
- [51] K. Binder and P. C. Hohenberg, *Phys. Rev. B* **6**, 3461 (1972).

- [52] C. P. Flynn, *Point Defects and Diffusion* (Charendon, Oxford, 1972).
- [53] J. R. Manning, *Diffusion Kinetics for Atoms in Crystals* (Van Nostrand, Princeton, 1968).
- [54] K. W. Kehr, K. Binder, and S. M. Reulein, *Phys. Rev. B* **39**, 4891 (1989).
- [55] K. Yaldram and K. Binder, *J. Stat. Phys.* **62**, 161 (1991); *Acta Metall.* **39**, 707 (1991); *Z. Phys. B* **82**, 405 (1991).
- [56] H. H. Kausch and M. Tirrell, *Annu. Rev. Mater. Sci.* **19**, 341 (1989).
- [57] K. Binder and H. Sillescu, in *Encyclopedia of Polymer Science and Engineering, Suppl. Vol.*, edited by J. E. Kroschwitz (Wiley, New York, 1989), p. 297.
- [58] K. Binder and D. Stauffer, *Phys. Rev. Lett.* **33**, 1006 (1974); *Z. Phys. B* **24**, 406 (1976).
- [59] I. M. Lifshitz and V. V. Slyozov, *J. Phys. Chem. Solids* **19**, 35 (1961).
- [60] Y. Oono and S. Puri, *Phys. Rev. Lett.* **58**, 836 (1987); *Phys. Rev. A* **38**, 434 (1988); S. Puri and Y. Oono, *ibid.* **38**, 1542 (1988).
- [61] T. M. Rogers, K. K. Elder, and R. C. Desai, *Phys. Rev. B* **37**, 196 (1988); A. Chakrabarti and J. D. Gunton, *ibid.* **37**, 3798 (1988).
- [62] D. Huse, *Phys. Rev. B* **34**, 7845 (1986).
- [63] C. Sagui, A. M. Somoza, C. Roland, and R. C. Desai, *J. Phys. A* **26**, L1163 (1993).
- [64] R. Pandit, M. Schick, and M. Wortis, *Phys. Rev. B* **25**, 5112 (1982).
- [65] K. Binder, *Phys. Rev. A* **29**, 341 (1984).
- [66] H.-O. Carmesin, D. W. Heermann, and K. Binder, *Z. Phys. B* **65**, 89 (1986).

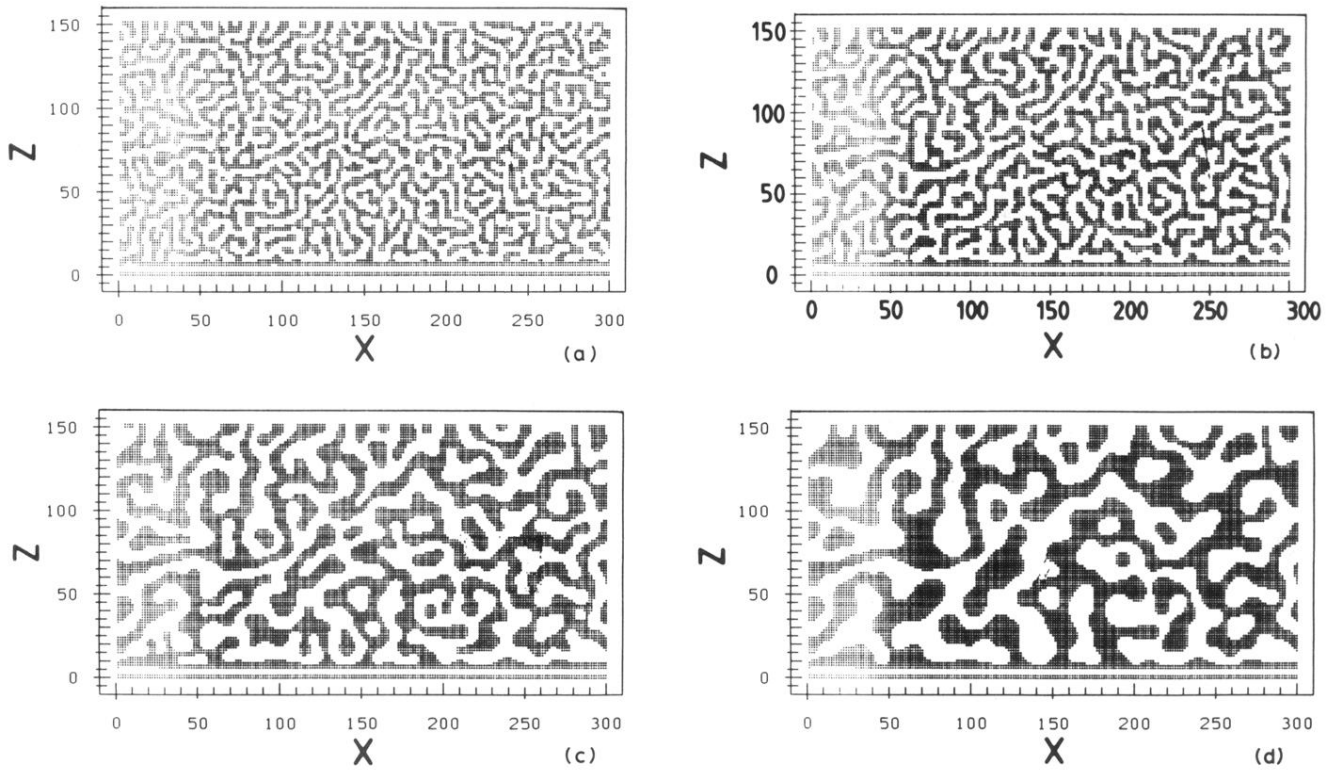


FIG. 10. Evolution pictures of our discrete implementation, analogous to Fig. 3, but for parameter values  $h_1=8$ ,  $g=-4$ , and  $\gamma=4$ , which correspond to a wet static equilibrium for the underlying continuum model (marked by a  $\times$  in Fig. 2).

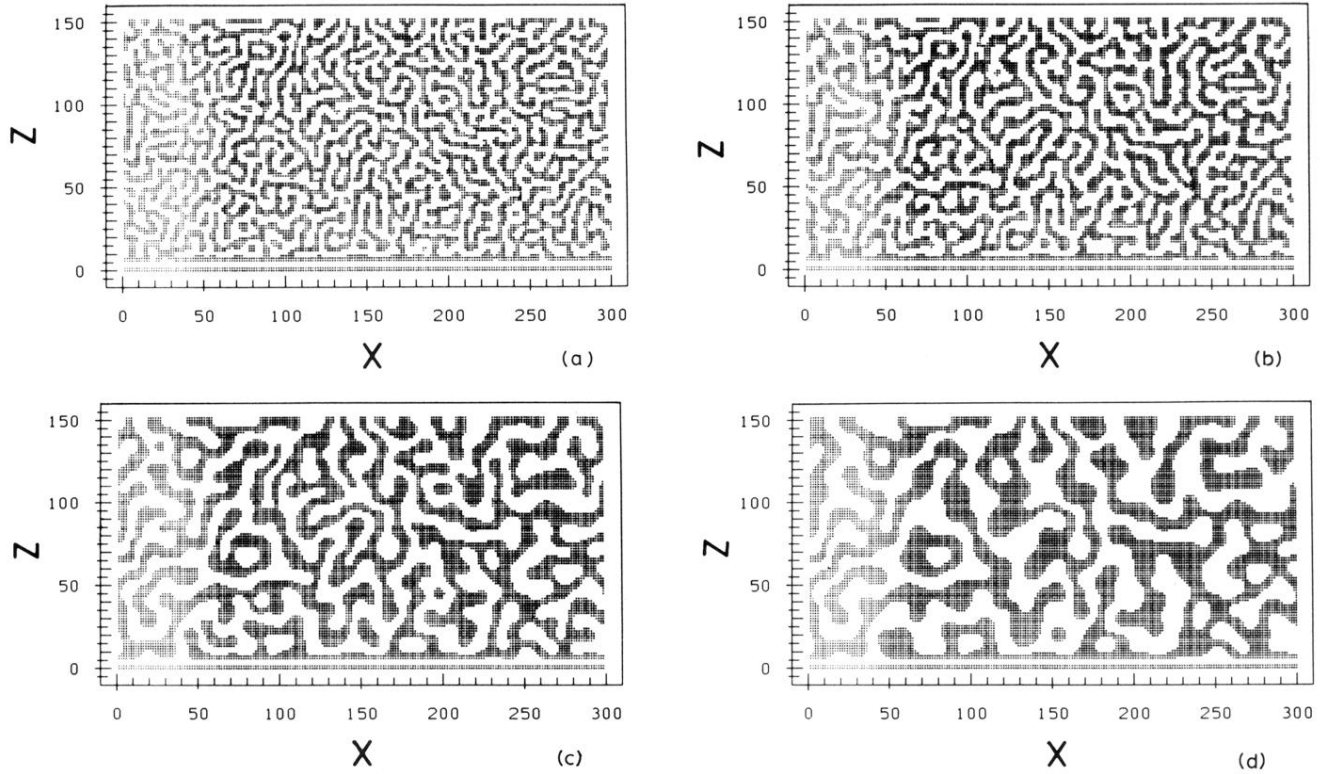


FIG. 3. Evolution pictures from our discrete implementation of the partial differential equation model with dynamical boundary conditions [Eqs. (13)–(15)] on a square lattice using Euler discretization with an isotropically discretized Laplacian. The discretization mesh sizes are  $\Delta\tau=0.05$  and  $\Delta X=1.5$  and our discrete model should be understood in terms of a cell-dynamical system (CDS) model which mimics the physics rather than the precise numerical solution of the partial differential equation. The lattice size is  $L_x \times L_z$  ( $L_x=300, L_z=150$ ) and the surface boundary conditions [Eqs. (14) and (15)] are applied at  $Z=0$ . Free boundary conditions are applied at  $Z=L_z$  and periodic boundary conditions are applied in the  $X$  direction. The parameter values are  $h_1=4$ ,  $g=-4$ , and  $\gamma=4$ , which correspond to a nonwet static equilibrium. The initial condition consists of uniformly distributed random fluctuations of amplitude  $\pm 0.025$  about a zero background, viz., a critical quench. Evolution pictures are shown for (a)  $\tau=50$ , (b)  $\tau=100$ , (c)  $\tau=500$ , and (d)  $\tau=4000$ .